NATIONAL ADVISORY COMMITTEE FOR AERONAUTICS

TECHNICAL NOTE 2362

TORSIONAL STRENGTH OF STIFFENED D-TUBES

By E. S. Kavanaugh and W. D. Drinkwater

University of Notre Dame

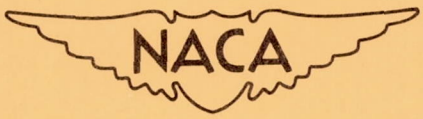

Washington
May 1951

NATIONAL ADVISORY COMMITTEE FOR AERONAUTICS

TECHNICAL NOTE 2362

TORSIONAL STRENGTH OF STIFFENED D-TUBES

By E. S. Kavanaugh and W. D. Drinkwater

SUMMARY

The present report covers a series of torsional tests on stiffened D-tubes of alclad 24S-T3 aluminum alloy having a cross section similar to the NACA 0012 airfoil section and a closing web at 30 percent of the chord. The stiffeners consisted of ribs and stringers. An average-strength chart has been developed for this type of structure that takes into account the skin thickness, rib spacing, and stringer spacing. This chart may also be used for unstiffened D-tubes.

Measurements of unit twist and unit strain were made at a number of points on most of the specimens. The unit-twist measurements indicated substantial agreement between this type of structure and Bredt's theory below the buckling point. The unit-strain measurements did not provide data that could be verified by theoretical analysis except for the strains measured in the webs.

INTRODUCTION

The primary object of this investigation has been the development of a chart that will permit the estimation of the ultimate torsional strength of stiffened D-sections. Nearly all airplanes use such a structure as a primary load-carrying member and an average-strength chart is considered to be quite desirable. With the advent of high-speed aircraft the use of symmetrical airfoils should become quite common and should enhance the value of this report. Other research projects on thin-shell sections have been carried out previously, as reported in references 1 and 2; however, only reference 1 deals with the pure torsion problem and the specimens tested did not have a closing web as is the case for the present investigation. Similar tests of a multi-flange box beam are reported in references 3 and 4.

Most of the previous work on structures of an elliptical or circular shape is based on an early investigation made by Donnell (reference 5) and many of the same factors reported therein were found to apply to this study.

Although reports on investigations of stiffened D-sections in torsion were not available, a similar study on stiffened circular cylinders was found in reference 6.

This investigation was conducted at the Structural Laboratory of the Department of Aeronautical Engineering, University of Notre Dame, under the sponsorship and with the financial assistance of the National Advisory Committee for Aeronautics.

SYMBOLS

A	area enclosed by section; 104.9 square inches
a	semimajor axis of section on basis of complete oval; 18 inches
E	modulus of elasticity of material; 10.2×10^6 psi
G	shear modulus of elasticity; 3.93×10^6 psi
L	distance between ribs, inches
S	actual skin length of largest panel in chordwise direction, inches
T	applied torsional moment, inch-pounds
T_u	applied torsional moment at failure, inch-pounds
α	angle of diagonal tension, degrees
θ	angle of twist per unit length, radians per inch
τ	torsional shearing stress, psi
τ_u	torsional shearing stress at ultimate moment, psi
$\tau_{u,c}$	calculated ultimate shearing stress, psi
$\tau_{u,e}$	experimental ultimate shearing stress, psi
μ	Poisson's ratio
t	thickness of skin, inches
s	parameter of section

SPECIMENS

The general layout of the specimens is shown in figure 1. This figure is a drawing of specimen 48. All other specimens are of the same general construction and size as specimen 48. As shown by table I, the main variables in this investigation were skin thickness, stringer spacing, and rib spacing. The first set of specimens, specimens 1 to 12, have variations in rib spacing of 8, 16, 24, and 48 inches and in skin thickness of 0.032, 0.051, and 0.072 inch. The remaining specimens have the same two variables with the addition of stringers to create smaller skin panels.

Figure 1 will apply to specimen 1 if all intermediate ribs, B to F, and all stringers are omitted; it applies similarly to any other specimen.

The rib thickness, web thickness, stringer size, and rivet size increased as the skin thickness increased. When ribs were omitted web stiffeners of the same section as the stringers for the given skin thickness were added to the web at the omitted rib station, making the web panel size constant regardless of actual number of ribs. Rivets one size larger than the skin rivets were used to attach the ribs and stiffeners to the web flange of the spar, one rivet for the 0.032- and 0.051-inch-skin specimens and two rivets for the 0.072-inch-skin specimen.

The stringers were continuous through rib notches. One side of the rib flange was offset and riveted to the flange of the stringer. When stringers were omitted the ribs were solid except for the lightening holes. Flanged lightening holes were used in all the ribs, their sizes being shown in figure 1.

The specimens were made according to normal aircraft manufacturing standards. The nose skin was formed to the leading-edge radius, and for the 0.051- and 0.072-inch-skin specimens the skin was rolled to match the rib contour. The nose sections of the ribs were hand-formed, the ribs heat-treated to the T3 condition, and the rib and hole flanges formed under a hydropress.

Standard aircraft tolerances were used throughout. The cross section of the various specimens was constant within the 1/32-inch tolerance. Although certain specimens were not constructed so carefully as might be desirable for theoretical investigations, there was no apparent effect on the ultimate strength. In a number of cases too much pressure was used in driving the rivets, and while this did not affect the ultimate strengths there is some question as to the effect on the initial buckling. The heavy rivet pressure left small dimpled areas around each rivet and in many cases initial wrinkles seemed to start from such an area.

All of the specimens were made with an NACA 0012 airfoil shape, and had a closing web at the 30-percent station, or 18 inches from the nose. The inside skin and web line was the mold line. This shape was chosen because it was thought to be a representative shape of the various airfoil sections used in the present design.

The stringer distribution used in the specimens simulated actual structural practice by placing more stringer area on one side, the assumed compression side, than on the other. An attempt was made to place the stringers so that each skin panel had the same buckling stress; however, this was not attained completely. A secondary reason for this stringer distribution was the desire to keep the number of rib types to a minimum.

The material used for the skin, web, and ribs was alclad 24S-T3 aluminum alloy. The grain of the skin was in the direction of the longitudinal axis of the specimens. The extrusions were made of 24S-T4 aluminum alloy. The rivets, type AN 456, were made of A17S-T4 aluminum alloy in the 1/8- and 5/32-inch sizes, and of 24S-T4 aluminum alloy in the 3/16-inch size.

Table II gives a listing of the ultimate stresses for a typical group of tensile coupons taken from the skin of the specimen. Some typical stress-strain curves are plotted in figure 2. In many of the curves the effects of the primary and secondary moduli are noticeable, although an average value of E appears to match the curves quite closely. This average value is 10.2×10^6 psi, which is suggested by reference 7 as a satisfactory value for 24S-T3 alclad sheet. While all of the data do not match this value, it is felt that experimental errors account for the deviation.

DESCRIPTION OF APPARATUS

The apparatus used to load the specimen in torsion is shown in figure 3. The test specimen was placed into the jig in a vertical position, rib A at the top, and leading edge at the left. The specimen was bolted to the steel angles 4 (see fig. 3) by a double row of AN 3 bolts, 72 in each end. These fittings were bolted to the top and bottom plates 1 and 2 by a single row of AN 5 bolts, 40 bolts in each plate spaced equally around the specimen.

The end fittings 4 were formed to the contour of the 0.072-inch-skin specimens; sheet filler strips were used to provide a match of the contour for the 0.032- and 0.051-inch-skin specimens. In all cases 0.072-inch filler strips were used for backing plates as is shown in section B-B of figure 1.

The load was applied to the bottom loading plate 2 by two hydraulic pistons 5. The $1\frac{1}{2}$-inch-diameter tension pistons are shown in figure 3. Another set of pistons having a $3\frac{1}{2}$-inch bore was used to obtain the maximum moment of 318,000 inch-pounds. These pistons were mounted in a manner that permitted movement in the horizontal and vertical planes so that no restraint was introduced by fixed pistons. Because of the pin joints at the ends of the pistons, the lower plate 2 was free to twist about any axis and no bending moments were introduced.

The pistons were operated by a hand pump 3, and pressure readings were taken from gages having a 0- to 600-psi range for one set of tests, and a 0- to 2000-psi range for the remaining set. A check of the load readings was made by strain gages mounted on the piston rods. These gages were diametrically opposed and were calibrated on a Baldwin-Southwark-Emery testing machine. The pistons were mounted to the loading fixture in planes 64 inches apart.

Baldwin-Southwark SR-4, types A-1, AR-1, and A-7 strain gages were used in the investigation. Two strain boxes 9, type K, and the Wheatstone bridge strain indicator were used, although most of the readings were made on the former. Three and four gang, eleven-position, radio switches were used in connecting the various strain gages to the strain box. Investigation disclosed a minimum change in contact resistance for the switches used.

Two rectangular frames 8 were used in conjunction with dial gages 6 and vertical columns 7 to obtain twist data. The frames were positioned in planes parallel to the ribs, the distance between the frames varying between 8 and 16 inches. The frames were used to measure twist in the middle of the specimen in order to eliminate any end effect. These frames were mounted by three pins, two in the web at a rib or stiffener station and one in the nose, the pointed ends in countersunk holes. The two web pins were held against the web by coiled springs. This manner of support was used to eliminate any local deflections due to skin or extrusion rotation. The extruded angles at the extreme ends of the frames 8 were in contact with the plungers of the dial gages 6 mounted on vertical columns 7 that rested on the floor. The vertical plane of these extrusions formed a continuation of the specimen chord plane, and the rotation of this plane was measured. The dial gages were graduated to read to the nearest 0.001 inch.

Two additional dial gages were mounted to the main jig at the ends of the hydraulic pistons. These were used to measure the rotation of the lower plate 2 of the specimen.

Stress-strain data were obtained on a Baldwin-Southwark-Emery machine for tensile coupons milled from sample skin strips. The extensometer used had a least count of 0.0001 inch.

TEST PROCEDURE

After the specimen and hydraulic pistons were bolted into place a few preliminary pressures were applied in an attempt to obtain accurate reference zeros for the measuring instruments and to check the operation of the equipment. Because of the small frictional forces present in the pistons, exact zeros were difficult to obtain, and with certain specimens, as indicated in figure 13, the true zero was found after plotting the twist data.

The loading increment was a function of the anticipated buckling load, and usually more readings were taken before buckling occurred than after buckling. At high loads the pressure was observed closely, as failure would sometimes occur abruptly, but for the most part the failing pressure did not drop off rapidly. The pressures after each increase in load were maintained constant until all the readings were obtained. At pressures close to 2000 psi this was difficult.

The dial gages on the frames 8 (fig. 3) were removed after definite wrinkling had occurred. This was done to prevent damage to the gage by any sudden failures occurring at the ultimate loads.

After the failing torque had been reached, one or two additional readings were usually taken. In each such instance the specimen was able to maintain a load of between 80 and 95 percent of the ultimate for considerable additional twist.

The pressure at which the first wrinkle was observed was recorded as the buckling load. The growth of the tension-field wrinkles was also observed visually and, on a number of specimens, the slope of the wrinkle was marked during the test.

PRECISION OF RESULTS

The hydraulic pistons used for loading the specimens were calibrated and checked four times during the testing program. This calibration included the pressure gages and the strain gages on the piston rods. The loading increments were read on the pressure gages, and the strain gages were used as a check of this indicated load and also as a check on the

equal distribution of the load between the two pistons. The moment applied by the large pistons was accurate to within 3.8 percent and that applied by the small pistons to within 2.6 percent.

The dial gages used for most of the measurements were read to the nearest 0.001 inch. As shown in figure 3, an additional set of dial gages accurate to the nearest 0.0001 inch was used in conjunction with the top set of gages for some of the tests. Twist readings of 5×10^{-6} radian per inch should have been possible with the dial gages accurate to 0.001 inch, but the scatter of the plotted points indicates that this accuracy was not attained. Part of the scatter was due to the inability to obtain accurate zero readings in some instances, and errors in the readings have caused a portion of this inaccuracy.

The strain gages mounted on the piston rods were found to be accurate to within 3 percent, this variation including possible errors in reading the pressure gages and the strain indicator.

RESULTS AND DISCUSSION

In order to provide the basic data, the strength of unstiffened cells was determined, and the additional strength contributed by stiffening members was subsequently investigated, which provided complete data for the section used.

Some previous tests of this nature have been made on sections with a circular or semielliptical contour, and, while the NACA 0012 airfoil used in the present investigation approaches a semielliptical contour, considerably more flat skin is present than was in the previous tests. While an exact correlation was not expected, the semielliptical design curve presented in reference 1 was used to predict the approximate failing loads for this test. A value of 5 was assumed for the ellipticity in this approximation. The presence of a closing web in the NACA 0012 specimens was a further complication in making the prediction. The loads calculated by this method were later found to be about 30 percent greater than the measured ultimate load. This could be expected on the basis of the differences in the nose radii, the NACA 0012 section having a much smaller semielliptical radius and a greater proportion of flat skin. While the specific values obtained in reference 1 could not be used directly, they were of value in a relative sense as the buckle patterns and failures of the unstiffened sections were quite similar to those of the present investigation.

The failing load in most cases was much greater than the buckling load. As the load was applied, the skin was observed carefully in an

effort to observe visually the initial wrinkle. This buckling point was recorded in all cases, but the wide scatter of the points leaves doubt as to their usefulness. Table III gives a tabulation of buckling torques and the corresponding shear stresses. In the case of the 0.032-inch-skin specimens the wrinkles appeared early; at times they were visible shortly after the initial loading. Although some of the scatter of the buckling points can be attributed to an initial waviness of the skin due to fabrication difficulty, the method of visual observation cannot be relied upon. The twist data were useful in some instances as a means of determining the buckling point. Many of the tests showed good agreement between the calculated change in slope of the twist curves after buckling, the assumed buckling point, and the observed buckling point. However, for the complete series of tests, the spread of the buckling points from 25 to 95 percent of the ultimate load has shown the observations to be of doubtful value. In one instance, the initial wrinkle did not occur until the ultimate load was applied, at which time the wrinkle appeared abruptly and a deep wrinkle was produced diagonally across the corners of the specimen. This specimen had a rib spacing of 48 inches and three stringers, one of which was on the side that buckled. The ultimate torques have shown some scatter, as is shown in figure 4, but the scatter fell well within anticipated limits.

The parameters used in reference 1 were thought to be a good starting point for development of the test data, and an ellipticity of 5 was assumed. Closer correlation was obtained using the parameters of reference 5 by changing the skin-thickness exponent from 2 to 1.75. Figure 5 shows all the experimental points plotted against these parameters, and, as was to be expected, the addition of stringers increased the ultimate strength. The parameters of figure 5 were multiplied by S^2, the square of the chordwise skin length of the largest skin panel (see table IV), to reduce the test data to an average curve that would apply to unstiffened as well as stiffened D-tubes. This curve is plotted as figure 4. A logarithmic relation was derived for this curve and the resulting equation is:

$$\left(1 - \mu^2\right)\frac{\tau_u L^2 S^2}{Et^{1.75}} = 3.24\left(\sqrt{1 - \mu^2}\,\frac{L^2 S^2}{2at}\right)^{0.74} \qquad (1)$$

The test values show best agreement with this equation at close rib spacings. The buckling characteristics of large unsupported skin panels in shear are difficult to evaluate in a precise manner and test results customarily show considerable scatter, as in figure 4.

The preceding equation (1) has been reduced to a simpler form for this series of tests and other, and possibly more useful, curves have been plotted as figure 6. The ultimate shear stress has been calculated from equation (1) and plotted against the L/t ratio for the different stringer combinations. In solving equation (1) for this stress the simplified form given below was used.

$$\tau_{u,c} = 2.506 \frac{t^{1.01}}{L^{0.52}s^{0.52}} \times 10^6 \text{ psi}$$

Table V shows a comparison between the calculated and experimental ultimate shear stresses. The deviation is most pronounced for the specimens having long unsupported skin panels, but the over-all average variation between the two values is about 1 percent.

Some unusual failures occurred which caused part of the deviation from the mean. As an example, specimen 22 took a higher load than specimen 34. The difference between the specimens was in the number of stringers, specimen 34 having seven stringers as compared with five for specimen 22. However, the plastic yielding of a rivet in a rib of specimen 34 permitted the wrinkle to cross the rib and thereby reduced the effective rigidity of the specimen. In a few cases the intersection of a stringer and rib was the point of failure, as shown in figure 7(a). The stringer rotated in the notch sufficiently to cause a bearing failure of the rib material. Figure 7(b) is a close-up view of this type of failure.

When the first rib failure of this type occurred, an attempt was made to eliminate such bearing failures by inserting gussets between the stringer and rib. These gussets are shown in figure 7(b). As is evidenced by this particular failure, the additional bearing area alone without a more rigid rib section was not successful. This failure was typical of the rib failures but not typical of the failures as a whole, six such failures having occurred. The failure in figure 7(b) was produced by continuing application of the load after the ultimate strength was reached. When these rib failures occurred, the ultimate load was lower than anticipated. It is possible that ribs of the same gage as the skin with smaller lightening holes would eliminate the rib failure.

The majority of the failures were produced by the collapse of the nose section. Figures 7(c), 7(d), and 8 illustrate this type of failure. Figure 8 illustrates the different patterns of the wrinkles at failure for the specimens without stringers. In all cases the initial wrinkle started near the beam and, as the load was increased, extended to within

about 1 inch of the nose, followed shortly by a collapse of the nose. As the wrinkles grew, the slope of the wrinkle changed until at failure it extended diagonally across the skin panel.

The nose collapse occurred in two ways. In one, as shown in the photograph in the upper right corner of figure 8, the initial wrinkle lengthened until it caused failure of the nose section. The photograph in the lower left corner of figure 8 shows the other type of failure, the initial wrinkle starting as before and increasing toward the leading edge until a second wrinkle developed below the initial wrinkle and extended into the nose, causing failure. This latter effect was most noticeable at the close rib spacings.

Figure 9 shows the development of the unit strain in the nose of three of the specimens. The gages recording this strain were mounted on the outside of the skin along the plane of symmetry. The discontinuity in the curve for specimen 10 occurred when one of the top nose panels buckled suddenly, although a greater torque was attained before the ultimate strength of the section was reached. The failure of specimen 7 did not occur abruptly and the unit-strain curves bear this out. These curves are for two gages mounted at opposite ends of the center nose panel at the same distance from adjacent ribs.

While this type of specimen was quite different from the type tested in reference 5, it is of interest to note the agreement between data for circular cylinders and for the unstiffened test specimens of this investigation. Figure 10 shows a comparison of these data, wherein the parameters for the circular and NACA 0012 sections are the same. There appears to be good agreement between the two tests. There is more scatter of the points than was found in the circular-cylinder tests, or in the semielliptical tests of reference 8, but the boundaries of the test points are about the same. The slope of the test points for a given rib spacing as shown in this figure is greater than the slope of Donnell's curve (reference 5). This is most apparent for the lowest set of three test points. By reducing the exponent of the skin thickness, the test points were brought into better agreement, as is shown by the bottom curve of figure 5.

The unit-twist data for all the specimens are given in table VI. The twist of the specimens was measured at three different planes. Two of the planes were taken near the center of the specimen, 8 or 16 inches apart depending upon the rib spacing, and the third at the bottom end. The data plotted in figures 11 to 14 were based upon the twist of the central portion of the specimen, the gage length being the distance between frames 8 shown in figure 3. Up to buckling, there was good agreement between the measured twist and the theoretical value calculated by Bredt's theory as presented in reference 9. Calculations were made

using the basic equation $\theta = T \oint \frac{ds}{t} \Big/ 4A^2G$ where the shear modulus was calculated from the experimentally verified value of 10.2×10^6 psi for Young's modulus, and Poisson's ratio taken as 0.33.

The measured and calculated values of unit twist are plotted in figure 11 for some of the specimens having no stringers. The effect on section rigidity of increasing the skin thickness is illustrated by figure 12, wherein the measured and calculated values again show agreement.

The data plotted in figure 13 reveal evident experimental error encountered during the testing program. The slopes of the measured and calculated twist curves agree although the experimental points do not originate at zero. The stiffness of the specimen is not affected by the addition of stringers, as indicated by figure 14. The slopes of the curves correspond, the principal change being an increase in the ultimate strength of the section. As the skin panel size is reduced, higher buckling stresses are carried by the plate, and, in turn, produce higher ultimate strength of the entire specimen. Review of reference 6 indicates a similarity between the torsional rigidity of stiffened circular sections and those of the current investigation.

An attempt was made to check the visual observation of buckling by plotting the over-all twist of the specimen as indicated by the rotation of the bottom loading plate. No exact correlation was obtained. The few cases which did check were not felt to be of sufficient consequence to warrant inclusion in this report, although table III shows buckling values for each specimen. One important result indicated by these data, however, was that the torsional rigidity of the center section was greater than that of the entire length. The conclusion was that the manner of introducing the load left something to be desired.

The design of the specimens provided a short length of skin extending beyond the end ribs, so as to eliminate end effect. Since the points at which failure occurred were well-distributed along the length of the specimen, it was felt that considerable success had been achieved in this regard. To provide an experimental check on the end effect, specimens of shorter length were tested. The points of failure and the ultimate strengths agreed well with those of the longer units.

In order to supply information as to the effect of minor variations of stringer area and/or rib thickness, several special cases were investigated. These specimens were identical with others in the series with the exception of the variable involved. For example, specimen 50 was built with lighter stringers than specimen 32. The ultimate strengths

of both specimens were substantially the same. In another trial, specimen 49 was supplied with heavier stringers than the otherwise identical specimen 31. Again, the results were in close agreement. While the small number of tests cannot establish validity of the results, the indication was that the size of the stringers was not the determining factor so far as the section strength was concerned. Specimens 56 and 57 were built with ribs of a heavier gage than the similar specimens 35 and 36, but again no appreciable change in ultimate strength was measured.

A number of gages were alined at the anticipated angle of the tension field. Figure 15 is a plot of the measured strain at a few of these points. As with some of the twist curves, good correlation with the visually observed buckling point was found, as indicated in the figure. The difference in buckling points indicated for specimen 4 was caused by the sequence in which the different skin panels on which the gages were mounted went into the buckled state.

The web strains in a few specimens were measured with rosette strain gages. Figure 16 is representative of these measurements. The calculated and measured shearing stresses are within 7 percent of agreement for the specimen plotted. Shearing-stress calculations were based on Bredt's first equation,

$$\tau = \frac{T}{2At}$$

Some strain information was taken from the gages mounted on the stringers, and plotted as shown in figure 17. The unit strain was found to be of small magnitude until buckling of the skin panels occurred. The flattening of the curves in both instances can be attributed to the appearance of definite wrinkles close to the stringers.

CONCLUDING REMARKS

The average ultimate strength in torsion can be calculated for stiffened or unstiffened D-tubes having a cross section similar to the NACA 0012 airfoil section and a closing web at 30 percent of the chord. The relationship involved in this calculation is:

$$\left(1 - \mu^2\right)\frac{\tau_u L^2 S^2}{Et^{1.75}} = 3.24\left(\sqrt{1 - \mu^2}\,\frac{L^2 S^2}{2at}\right)^{0.74}$$

where

μ	Poisson's ratio
τ_u	torsional shearing stress at ultimate moment, inch-pounds
L	distance between ribs, inches
S	actual skin length of largest panel in chordwise direction, inches
E	modulus of elasticity of material; 10.2×10^6 psi
t	thickness of skin, inches
a	semimajor axis of section on basis of complete oval; 18 inches

The average-ultimate-strength curve presented in this report and based on the above equation should be useful in determining the ultimate load-carrying ability of this type of structure. With the advent of high-speed aircraft the use of symmetrical airfoils should become quite common and should enhance the value of the report.

Comparison of the measured twist with Bredt's theory has shown good agreement below the buckling point, although the buckling point itself was not well-defined.

University of Notre Dame
Notre Dame, Ind., June 11, 1948

REFERENCES

1. Sechler, E. E., and Frederick, J. L.: The Strength of Semielliptical Cylinders Subjected to Combined Loadings. NACA TN 957, 1945.

2. Sherwood, A. W.: The Strength of Thin-Wall Cylinders of a D Cross Section in Combined Pure Bending and Torsion. NACA TN 904, 1943.

3. Levy, Samuel, McPherson, Albert E., and Ramberg, Walter: Torsion Test of a Monocoque Box. NACA TN 872, 1942.

4. McPherson, A. E., Goldenberg, D., and Zibritosky, G.: Torsion Test to Failure of a Monocoque Box. NACA TN 953, 1944.

5. Donnell, L. H.: Stability of Thin-Walled Tubes under Torsion. NACA Rep. 479, 1933.

6. Moore, R. L., and Wescoat, C.: Torsion Tests of Stiffened Circular Cylinders. NACA ARR 4E31, 1944.

7. Anon.: Strength of Aircraft Elements. ANC-5, U. S. Govt. Printing Office, 1942.

8. Lundquist, Eugene E., and Burke, Walter F.: Strength Tests of Thin-Walled Duralumin Cylinders of Elliptic Section. NACA TN 527, 1935.

9. Timoshenko, S.: Theory of Elasticity. McGraw-Hill Book Co., Inc., 1934.

TABLE I

DIMENSIONS OF SPECIMENS USED IN TORSION TESTS OF STIFFENED D-TUBES

Specimen	Web thickness (in.) (1)	Skin thickness (in.) (1)	Rib spacing (in.) (2)	Rib thickness (in.)	Stringer position (3)	Stringer area (sq in.) (4)	Flange area (sq in.) (5)	Rivet diameter (in.)
Over-all length, 52 in.								
1	0.04	0.032	48	0.025	None	0	0.107	1/8
2	.064	.051	48	.040		0	.183	5/32
3	.081	.072	48	.064		0	.277	3/16
4	.04	.032	24	.025		0	.107	1/8
5	.064	.051	24	.040		0	.183	5/32
6	.081	.072	24	.064		0	.277	3/16
7	.04	.032	16	.025		0	.107	1/8
8	.064	.051	16	.040		0	.183	5/32
9	.081	.072	16	.064		0	.277	3/16
10	.040	.032	8	.025		0	.107	1/8
11	.064	.051	8	.040		0	.183	5/32
12	.081	.072	8	.064		0	.277	3/16
13	0.040	0.032	48	0.025	2,4,8	0.085	0.107	1/8
14	.064	.051	48	.040		.127	.183	5/32
15	.081	.072	48	.064		.172	.277	3/16
16	.040	.032	24	.025		.085	.107	1/8
17	.064	.051	24	.040		.127	.183	5/32
18	.081	.072	24	.064		.172	.277	3/16
19	.040	.032	16	.025		.085	.107	1/8
20	.064	.051	16	.040		.127	.183	5/32
21	.081	.072	16	.064		.172	.277	3/16
22	.040	.032	8	.025		.085	.107	1/8
23	.064	.051	8	.040		.127	.183	5/32
24	.081	.072	8	.064		.172	.277	3/16
25	0.040	0.032	48	0.025	2,3,4,7,8	0.085	0.107	1/8
26	.064	.051	48	.040		.127	.183	5/32
27	.081	.072	48	.064		.172	.277	3/16
28	.040	.032	24	.025		.085	.107	1/8
29	.064	.051	24	.040		.127	.183	5/32
30	.081	.072	24	.064		.172	.277	3/16
31	.040	.032	16	.025		.085	.107	1/8
32	.064	.051	16	.040		.127	.183	5/32
33	.081	.072	16	.064		.172	.277	3/16
34	.040	.032	8	.025		.085	.107	1/8
35	.064	.051	8	.040		.127	.183	5/32
36	.081	.072	8	.064		.172	.277	3/16
37	0.040	0.032	48	0.025	1,2,3,4,7,8,9	0.085	0.107	1/8
38	.064	.051	48	.040		.127	.183	5/32
39	.081	.072	48	.064		.172	.277	3/16
40	.040	.032	24	.025		.085	.107	1/8
41	.064	.051	24	.040		.127	.183	5/32
43	.040	.032	16	.025		.085	.107	1/8
44	.064	.051	16	.040		.127	.183	5/32
45	.081	.072	16	.064		.154	.277	3/16
46	.040	.032	8	.025		.085	.107	1/8
47	.051	.051	8	.040		.127	.183	5/32
48	.081	.072	8	.064		.154	.277	3/16
49	0.040	0.032	16	0.025	2,3,4,7,8	0.127	0.183	5/32
50	.064	.051	16	.040		.085	.107	1/8
51	.081	.072	16	.064		.127	.183	5/32
Over-all length, 36 in.								
52	0.040	0.032	8	0.025	2,3,4,7,8	0.085	0.107	1/8
53	.064	.051	8	.040		.127	.183	5/32
54	.081	.072	8	.064		.154	.277	3/16
Over-all length, 28 in.								
55	0.040	0.032	8	0.025	2,3,4,7,8	0.085	0.107	1/8
56	.064	.051	8	.064		.127	.183	5/32
57	.081	.072	8	.072		.154	.277	3/16

[1]Web and skin were made of alclad 24S-T3 aluminum alloy.

[2]When ribs were 48 in. apart, rib positions A and G were used; when ribs were 24 in. apart, rib positions A, D, and G were used; when ribs were 16 in. apart, rib positions A, C, E, and G were used; and when ribs were 8 in. apart, rib positions A, B, C, D, E, F, and G were used.

[3]Stringers were made of 24S-T3 aluminum-alloy extrusions. Numbers in column refer to positions marked in fig. 1.

[4]The areas and AN standard drawing numbers are as follows: 0.085 sq in., AN 10135-0701; 0.127 sq in., AN 10135-1002; and 0.172 sq in., AN 10135-1004. Stringer section with area of 0.154 sq in. was $1\frac{1}{8}$ by $\frac{11}{16}$ by 0.084 in. and had a bulb-angle flat top.

[5]Flanges were in positions 5 and 6 (see fig. 1).

TABLE II

TYPICAL ULTIMATE TENSILE STRESSES OF ALCLAD 24S-T3

ALUMINUM-ALLOY SKIN MATERIAL

[Tensile load applied with grain]

Specimen from which coupon taken	Thickness of coupon (in.)	Ultimate tensile stress (psi)
2	0.048	66,500
3	.070	66,900
4	.032	65,000
8	.049	68,200
11	.049	65,500
14	.049	67,300
16	.032	65,200
22	.049	66,500
23	.048	67,100

TABLE III

VISUALLY OBSERVED TORSIONAL BUCKLING MOMENTS AND SHEAR STRESSES OF STIFFENED D-TUBES OF ALCLAD 24S-T3 ALUMINUM ALLOY

[$\mu = 0.33$; $E = 10.2 \times 10^6$ psi; $a = 18$ in.]

Specimen	Buckling torque, T_{cr} (in-lb)	Shear stress at buckling (psi)	Specimen	Buckling torque, T_{cr} (in-lb)	Shear stress at buckling (psi)
1	6.0×10^3	920	30	129.0×10^3	8,650
2	19.3	1875	31	25.0	3,720
3	41.5	2780	32	51.0	5,060
4	7.4	1210	33	148.0	9,950
5	13.0	1260	34	26.0	3,870
6	53.1	3560	35	57.5	5,700
7	8.4	1380	36	182.5	12,200
8	10.3	1000	37	21.0	3,220
9	53.0	3550	38	43.5	4,220
10	12.1	1860	39	94.1	6,220
11	32.0	3110	40	24.8	3,810
12	75.5	5050	41	61.5	5,970
13	8.4	1250	42	----------	------
14	19.3	1870	43	30.0	4,600
15	57.0	3770	44	75.5	7,330
16	6.7	1030	45	145.0	9,600
17	24.5	2430	46	34.5	5,300
18	39.5	2610	47	85.2	8,300
19	12.1	1800	48	195.0	12,900
20	26.0	2520	49	28.5	4,370
21	52.5	3520	50	53.0	5,150
22	12.5	1860	51	154.0	10,200
23	38.7	3690	52	17.4	2,590
24	92.5	6200	53	57.6	5,590
25	17.4	2670	54	145	9,600
26	44.2	4290	55	26.5	3,940
27	94.2	6300	56	57.6	5,600
28	19.3	2870	57	134	8,870
29	59.4	5890			

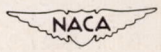

TABLE IV

TORSIONAL STRENGTH OF STIFFENED D-SECTIONS OF ALCLAD 24S-T3 ALUMINUM ALLOY

[$E = 10.2 \times 10^6$ psi; $\mu = 0.33$; $a = 18$ in.]

Specimen	L (in.)	t (in.)	S (in.)	T (in-lb)	$\frac{(1-\mu^2)\tau_u L^2 S^2}{Et^{1.75}}$	$\frac{(1-\mu^2)^{1/2} L^2 S^2}{2at}$	$\frac{(1-\mu^2)\tau_u L^2}{Et^{1.75}}$	$\frac{(1-\mu^2)^{1/2} L^2}{2at}$	$\frac{(1-\mu^2)\tau_u L^2}{Et^2}$
1	48	0.031	19.7	9,100	47,400	756,000	122.10	1948	322.5
2	48	.049	19.7	22,000	32,550	478,000	83.89	1232	178.5
3	48	.071	19.9	53,800	29,400	337,000	74.20	852	143.2
4	24	.029	19.7	16,500	26,150	202,000	66.04	510	161.0
5	24	.049	19.7	43,300	16,040	119,400	40.51	301.5	87.9
6	24	.071	19.9	77,000	10,520	84,200	26.57	212.6	51.4
7	16	.029	19.7	22,000	15,480	89,800	39.90	231	95.6
8	16	.049	19.7	50,600	8,330	53,100	21.45	136.8	45.6
9	16	.071	19.9	119,500	7,250	37,400	18.32	94.6	35.5
10	8	.031	19.7	36,800	5,330	21,000	13.73	54.2	33.0
11	8	.049	19.7	85,200	3,500	13,270	9.04	34.2	19.2
12	8	.071	19.9	183,500	2,786	9,350	7.04	23.6	13.6
13	48	.032	11.4	18,400	28,600	245,000	220.00	188.5	-----
14	48	.049	11.4	40,900	20,300	160,500	156.00	1234	-----
15	48	.072	11.9	74,100	14,000	119,200	98.60	848	-----
16	24	.031	11.4	31,600	13,780	63,200	106.00	487	-----
17	24	.048	11.4	62,900	8,260	40,800	63.50	314	-----
18	24	.072	11.9	140,000	6,600	29,700	46.50	209	-----
19	16	.032	11.4	42,800	7,400	27,200	56.90	209	-----
20	16	.049	11.4	87,500	4,810	17,800	37.00	137	-----
21	16	.071	11.9	188,000	4,090	13,420	28.80	94.6	-----
22	8	.032	11.4	58,100	2,500	6,810	19.25	52.3	-----
23	8	.050	11.4	117,500	1,535	4,360	11.80	33.6	-----
24	8	.071	11.9	261,000	1,420	3,360	10.00	23.6	-----
25	48	.031	8.4	24,800	23,500	137,400	333.00	1946	-----
26	48	.049	8.4	58,500	15,780	86,900	223.50	1230	-----
27	48	.071	8.9	123,200	13,440	67,300	169.8	850	-----
28	24	.032	8.4	40,500	8,550	33,200	120.8	472	-----
29	24	.048	8.4	78,000	5,550	22,150	78.7	314	-----
30	24	.071	8.9	167,000	4,550	16,800	57.6	213	-----
31	16	.032	8.4	48,500	4,550	14,800	64.5	209	-----
32	16	.048	8.4	96,500	3,050	9,870	43.3	139.6	-----
33	16	.071	8.9	199,000	2,410	7,470	30.5	94.5	-----
34	8	.032	8.4	57,700	1,350	3,700	19.14	52.5	-----
35	8	.048	8.4	129,700	1,027	2,470	14.58	34.9	-----
36	8	.071	8.9	27,800	842	1,870	10.62	23.6	-----
37	48	.031	6.1	33,800	16,900	72,600	455.00	1948	-----
38	48	.049	6.2	63,100	9,260	47,300	241.00	1232	-----
39	48	.072	6.6	125,200	7,260	36,500	166.00	848	-----
40	24	.031	6.1	52,100	6,500	18,100	175.00	487	-----
41	24	.049	6.2	114,000	4,180	11,820	108.80	308	-----
43	16	.031	6.1	60,100	3,330	8,040	89.60	216	-----
44	16	.049	6.2	128,900	2,100	5,260	54.70	137	-----
45	16	.072	6.6	256,000	1,645	4,060	37.80	93.2	-----
46	8	.031	6.1	78,000	1,080	2,010	29.10	54.1	-----
47	8	.049	6.2	162,300	662	1,315	17.20	34.3	-----
48	8	.072	6.6	318,000	512	1,015	11.70	23.3	-----
49	16	.031	8.4	47,000	4,940	15,300	70.00	216	-----
50	16	.049	8.4	912,000	2,725	9,660	38.60	137	-----
51	16	.072	8.4	202,000	2,105	6,580	29.80	93	-----
52	8	.032	8.4	51,300	1,200	3,700	17.10	52.4	-----
53	8	.049	8.4	132,500	991	2,415	14.05	34.2	-----
54	8	.072	8.4	272,000	711	1,644	10.06	23.3	-----
55	8	.032	8.4	60,200	1,410	3,700	19.90	52.4	-----
56	8	.049	8.4	130,000	974	2,410	13.80	34.2	-----
57	8	.072	8.4	270,000	704	1,644	9.97	23.3	-----

TABLE V

COMPARISON OF EXPERIMENTAL AND CALCULATED ULTIMATE SHEAR STRESS OF STIFFENED D-TUBES OF ALCLAD 24S-T3 ALUMINUM ALLOY

Specimen	Calculated ultimate shear stress, $\tau_{u,c}$ (psi) (1)	Experimental ultimate shear stress, $\tau_{u,e}$ (psi)	$\frac{L}{t}$	Specimen	Calculated ultimate shear stress, $\tau_{u,c}$ (psi) (1)	Experimental ultimate shear stress, $\tau_{u,e}$ (psi)	$\frac{L}{t}$
1	2,130	1,396	1548	29	7,390	7,720	500
2	3,410	2,135	980	30	10,700	11,200	338
3	4,930	3,610	677	31	6,040	7,220	500
4	2,855	2,710	828	32	9,150	9,570	333
5	4,880	4,210	490	33	13,250	13,300	225
6	7,050	5,160	338	34	8,650	8,580	250
7	3,530	3,610	553	35	13,150	12,850	166
8	6,020	4,910	327	36	19,000	18,600	112
9	8,750	8,020	225	37	3,900	5,180	1548
10	5,390	5,650	258	38	6,210	6,130	980
11	8,650	8,270	163	39	8,850	8,290	667
12	12,500	12,300	112	40	5,570	8,000	775
13	2,910	2,735	1496	41	8,900	11,080	490
14	4,510	3,970	980	42	------	------	----
15	6,500	4,900	667	43	6,900	9,220	517
16	4,020	4,850	775	44	11,000	12,500	327
17	6,330	6,240	500	45	15,650	16,950	222
18	9,300	9,280	333	46	9,930	12,000	258
19	5,140	6,370	500	47	15,800	15,750	163
20	7,980	8,480	327	48	22,400	21,000	111
21	11,350	12,600	225	49	5,850	7,210	517
22	7,390	8,650	250	50	9,400	8,850	327
23	11,650	11,200	160	51	13,800	13,380	222
24	16,350	17,500	112	52	8,650	7,650	250
25	3,300	3,810	1548	53	13,400	12,880	163
26	5,280	5,670	980	54	19,700	18,000	111
27	7,480	8,270	677	55	8,650	8,950	250
28	4,880	6,030	750	56	13,400	12,620	163
				57	19,700	17,850	111

(1) $\tau_{u,c} = 2.506 \frac{t^{1.01}}{L^{0.52} S^{0.52}} \times 10^6$ psi.

TABLE VI

UNIT TWIST DATA FOR STIFFENED D-TUBES WITH NACA 0012 SECTION

[Specimens made of alclad 24S-T3 aluminum alloy; $E = 10.2 \times 10^6$ psi, $\mu = 0.33$, $a = 18$ in.]

Torsional moment (in-lb)	Unit twist (radian/in.) for specimen -							
	1 (1)	1 (2)	4 (1) (3)	4 (2) (3)	7 (1)	7 (2)	10 (1)	10 (2)
0	0	0	0	0	0	0	0	0
$.15 \times 10^4$	0	0	0	$.198 \times 10^{-4}$	----------	----------	$.222 \times 10^{-4}$	$.276 \times 10^{-4}$
.31	0	$.470 \times 10^{-4}$	0	.396	$.466 \times 10^{-4}$	$.386 \times 10^{-4}$	.571	.378
.48	0	.680	0	.692	.709	.520	.844	.585
.67	$.282 \times 10^{-4}$	1.110	$.751 \times 10^{-4}$	1.055	.898	.722	.944	.688
.75	.376	1.410	.751	1.187	----------	----------	----------	----------
.84	.751	1.920	.850	1.417	1.097	1.041	1.097	.843
.93			1.408	1.714	----------	----------	----------	----------
1.03			1.690	2.044	1.472	1.477	1.268	.998
1.12			2.066	2.373	----------	----------	----------	----------
1.21			2.629	2.736	1.821	1.931	1.409	1.152
1.29			3.381	3.030	----------	----------	----------	----------
1.38			4.132	3.954	2.296	2.401	1.611	1.359
1.47			5.259	4.807	----------	----------	----------	----------
1.56			6.573	5.596	2.698	2.876	1.836	1.583
1.65					3.011	3.291	----------	----------
1.74					3.324	3.659	2.085	1.996
1.84					3.720	4.114	----------	----------
1.93					4.234	4.886	2.377	2.151
2.03					4.477	5.574	2.533	2.271
2.12						6.213	2.689	2.375
2.20							2.789	2.668
2.29							2.939	2.753
2.38							3.092	2.856
2.48							3.275	2.994
2.55							3.462	3.114
2.66							3.654	3.338
2.75							3.849	3.579
2.84							4.015	3.734
2.93							4.234	3.923
3.03							4.580	4.267
3.12							5.054	4.508
3.22							5.157	4.851
3.30							5.445	5.144
3.40							6.091	4.622
3.50								6.242
3.58								6.689
3.68								8.861
	2 (1)	2 (2)	3 (1) (3)	3 (2) (3)	5 (1)	5 (2)	8 (1)	8 (2)
0	0	0	0	0	0	0	0	0
$.15 \times 10^4$	$.240 \times 10^{-4}$	$.073 \times 10^{-4}$	$.090 \times 10^{-4}$	$.087 \times 10^{-4}$	$.126 \times 10^{-4}$	$.236 \times 10^{-4}$	0	$.115 \times 10^{-4}$
.31	.270	.147	.141	.133	.222	.464	$.084 \times 10^{-4}$	.191
.48	.440	.350	.201	.121	.292	.439	.171	.234
.67	.480	.410	.267	.226	.394	.556	.261	.330
.84	.610	.502	.340	.251	.478	.606	.361	.412
1.03	.660	.586	.403	.307	.589	.789	.442	.511
1.21	.800	.634	.475	.368	.712	1.058	.574	.628
1.56	.980	.738	.622	.477	1.016	1.439	.841	.828
1.74	1.140	.933	.700	.529	1.217	1.760	----------	----------
1.93	1.340	1.138	.769	.592	1.629	2.320	1.112	.986
2.12	1.750	1.667	.847	.580	1.767	2.537	----------	----------
2.29			.929	.694	2.088	3.309	1.442	1.458
2.48			1.010	.756	2.819	3.823	----------	----------
2.66			1.094	.786	3.360	4.139	1.794	3.206
2.84			1.181	.803	3.492	4.578	----------	----------
3.03			1.256	.902	4.054	3.309	2.266	
3.12			----------	----------	4.508		----------	
3.22			1.346	.964	4.886		----------	
3.40			1.424	1.051	5.649		2.987	
3.58			1.512	1.085			----------	
3.76			1.611	1.156			4.060	
3.96			1.707	1.230			----------	
4.15			1.830	1.289			4.967	
4.34			2.055	1.462			----------	
4.51			2.260				5.725	
4.68			2.437				----------	
4.88			2.723				6.569	
5.08			3.092					
5.28			3.573					

[1]Gage length taken as entire length of specimen.
[2]Gage length taken in middle of specimen.
[3]Questionable data.

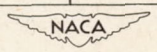

TABLE VI

UNIT-TWIST DATA FOR STIFFENED D-TUBES WITH NACA 0012 SECTION - Continued

Torsional moment (in-lb)	Unit twist (radian/in.) for specimen -							
	6 (1)	6 (2)	9 (1)	9 (2)	11 (1)	11 (2)	12 (1)	12 (2)
0	0	0	0	0	0	0	0	0
$.04 \times 10^4$					$.042 \times 10^{-4}$	$.007 \times 10^{-4}$		
.07					.156	.178		
.30	$.033 \times 10^{-4}$	$.210 \times 10^{-4}$	$.180 \times 10^{-4}$	$.225 \times 10^{-4}$	.270	.234	$.175 \times 10^{-4}$	$.325 \times 10^{-4}$
.52					.373	.341		
.75	.243	.340	.332	.381	.469	.408		
.98					.619	.515		
1.18	.382	.510	.528	.556	.739	.657	.534	.525
1.38					.877	.773		
1.61	.583	.690	.751	.731	1.004	.857		
1.86					1.136	.987		
2.06	.838	.860	.942	.875	1.268	1.119	.973	.863
2.26					1.388	1.236		
2.51	1.016	.990	1.125	1.038	1.506	1.341		
2.74					1.617	1.400		
2.91	1.160	1.160	1.286	1.137	1.698	1.474	1.342	1.187
3.15					1.888	1.664		
3.39	1.340	1.370	1.555	1.363	2.055	1.802		
3.62					2.218			
3.80	1.536	1.540	1.823	1.569	2.371		1.875	1.560
4.28	1.737	1.740	2.036	1.738	2.708			
4.70	1.899	1.920	2.265	1.888	3.089		2.346	1.910
5.15	2.164	2.090	2.448	1.994	3.402		2.517	2.050
5.59	2.407	2.470	2.781	2.219	3.991		2.755	2.230
6.05	3.191	2.770	3.125	2.444	4.553		2.988	2.380
6.47	4.081	3.560	3.478	2.738	5.229		3.242	2.530
6.96	4.550	3.970	3.894	3.088	5.030		3.475	2.700
7.40	5.508	4.490	4.265	3.413	6.356		3.688	2.930
7.90			4.913	3.919	7.107		3.969	3.050
8.33			5.565	4.475	9.926		4.198	3.290
8.82			6.275	4.819			4.419	3.250
9.28			6.930				5.315	3.600
9.76			7.682				4.913	3.790
10.20			8.621				5.157	3.990
10.67			9.373					
11.13			11.109				6.101	4.330
11.59			14.144					
12.05							6.667	4.863
12.98							7.319	
13.88							8.076	
14.84							8.828	
15.78							9.578	
16.80							12.015	

	13 (1)	13 (2)	14 (1)	14 (2)	16 (1) (3)	16 (2) (3)	19 (1)	19 (2)
0	0	0	0	0	0	0	0	0
$.150 \times 10^4$	$.171 \times 10^{-4}$	$.109 \times 10^{-4}$			$.182 \times 10^{-4}$	$.180 \times 10^{-4}$	$.188 \times 10^{-4}$	$.398 \times 10^{-4}$
.310	.207	.347			.306	.248	.282	.103
.480	.466	.298	$.282 \times 10^{-4}$	$.204 \times 10^{-4}$	.453	.521	.423	.361
.670	.598	.345	.376	.306	.592	.674	.517	.506
.840	.679	.519	.517	.362		1.042	.704	.645
1.025	1.034	.708	.611	.424	1.074	1.272	.892	.789
1.210	1.409	.991	.704	.501	1.319	1.499	1.033	.974
1.380	1.872	1.504	.798	.574	1.645	1.807	1.315	1.305
1.560	2.542	2.002	.892	.638	1.889	1.685	1.549	1.482
1.740	3.621	4.534	.986	.722	2.151	2.000	1.597	1.731
1.930			1.127	.808	2.428	2.307	2.066	2.002
2.120			1.315	.907	2.790	2.615	2.348	2.257
2.290			1.409	1.001		3.332	2.676	2.612
2.475			1.549	1.111	4.276	4.465	3.052	2.964
2.660			1.690	1.261		4.898	3.521	3.590
2.840			1.878	1.399		5.759	3.991	4.123
3.025			2.019	1.553		6.669	4.461	4.548
3.220							4.977	4.966
3.400			2.583	1.003			5.447	5.457
3.580							5.963	5.991
3.760			3.287	2.697				
3.950			5.447	4.624			9.954	
4.140							11.644	

[1]Gage length taken as entire length of specimen.
[2]Gage length taken in middle of specimen.
[3]Questionable data.

TABLE VI

UNIT-TWIST DATA FOR STIFFENED D-TUBES WITH NACA 0012 SECTION - Continued

Torsional moment (in-lb)	Unit twist (radian/in.) for specimen -							
	15 (1)	15 (2)	17 (1)	17 (2)	18 (1)	18 (2)	20 (1)	20 (2)
0	0	0	0	0	0	0	0	0
$.30 \times 10^4$	$.179 \times 10^{-4}$	$.114 \times 10^{-4}$	$.375 \times 10^{-4}$	$.660 \times 10^{-4}$	$.166 \times 10^{-4}$	$.313 \times 10^{-4}$	$.659 \times 10^{-4}$	$.388 \times 10^{-4}$
.52	---	---	.469	.780	---	---	.751	.500
.75	---	---	.657	1.010	---	---	.938	.564
.98	---	---	.751	1.190	---	---	1.032	.650
1.18	.536	.434	.844	1.160	.514	.553	1.221	.781
1.38	---	---	1.032	1.310	---	---	1.320	.888
1.61	---	---	1.126	1.350	---	---	1.410	1.025
1.86	---	---	1.315	1.340	---	---	1.590	1.138
2.06	.910	.578	1.440	1.440	.901	1.099	1.780	1.238
2.26	---	---	1.596	1.550	---	---	1.880	1.369
2.51	---	---	1.784	1.780	---	---	2.070	1.525
2.74	---	---	---	---	---	---	2.540	1.600
2.91	1.258	.996	2.011	1.960	1.219	1.073	2.530	1.725
3.39	1.536	1.224	2.523	2.590	---	---	2.720	2.144
3.80	1.722	1.394	3.005	2.900	1.683	1.595	3.010	2.513
4.28	1.954	1.749	3.569	3.630	---	---	3.380	2.868
4.70	2.196	1.754	4.130	4.380	2.159	1.948	4.040	3.156
5.15	2.340	1.855	4.546	4.930	2.349	2.075	4.230	3.338
5.59	2.606	2.074	5.259	5.680	2.593	2.253	4.880	4.181
6.05	2.847	2.259	7.794	12.800	2.846	2.410	5.350	4.763
6.47	3.194	2.443			3.140	2.568	6.380	5.063
6.96	3.714	2.995			3.389	2.704	7.510	6.563
7.40					3.678	3.041	8.450	6.906
7.90					3.991	3.203	10.610	
8.33					4.388	3.835	12.670	
8.82					4.677	4.079		
9.28					4.948	4.309		
9.76					5.441	4.697		
	21 (1)	21 (2)	24 (1)	24 (2)	33 (1)	33 (2)	51 (1) (3)	51 (2) (3)
0	0	0	0	0	0	0	0	0
$.75 \times 10^4$	$.556 \times 10^{-4}$	$.485 \times 10^{-4}$	---	---	$.42 \times 10^{-4}$	$.370 \times 10^{-4}$	$.637 \times 10^{-4}$	$.601 \times 10^{-4}$
2.00	.911	.851	1.286×10^{-4}	$.729 \times 10^{-4}$	.79	.734	1.055	1.001
3.35	1.463	1.193	---	---	1.17	1.132	1.472	1.363
4.60	1.899	1.480	2.057	1.229	1.61	1.453	2.001	1.813
5.70	2.215	1.906	---	---	2.04	1.825	2.566	2.141
6.75	3.044	2.311	2.863	1.940	2.50	2.167	3.149	2.375
7.75	3.696	2.803	---	---	3.02	2.527	3.783	2.930
8.75	4.384	3.288	3.520	2.724	3.64	2.944	4.321	3.334
9.90	5.072	3.761	4.051	3.103	4.19	3.335	4.928	3.709
11.00	5.812	4.283	4.609	3.530	4.74	3.742	5.472	4.092
12.00	6.629	4.933	5.212	3.966	5.36	4.162	6.112	4.556
13.00	7.561	5.702	5.823	4.375	5.98	4.581	6.647	4.954
14.00	8.498	6.404	6.218	4.853	6.79	4.965	7.371	5.404
15.00	9.766	8.549	7.015	5.323	7.32	5.409	8.219	5.874
16.20	11.786	10.236	7.887	5.884	7.98	5.800	9.249	6.588
17.25	14.836		8.545	6.329	8.59	6.210	10.049	7.074
18.25	18.640		9.390	6.826	9.16	6.592	12.161	10.328
18.75	20.707		---	---	11.17	6.510	14.039	
19.25			10.094	7.452	12.72			
20.25			10.892	8.081				
22.50			12.864	9.665				
24.50			15.963					
	22 (1) (3)	22 (2) (3)	23 (1)	23 (2)	26 (1)	26 (2)	27 (1)	27 (2)
0	0	0	0	0	0	0	0	0
$.30 \times 10^4$	$.375 \times 10^{-4}$	$.199 \times 10^{-4}$	$.845 \times 10^{-4}$	---	$.282 \times 10^{-4}$	$.203 \times 10^{-4}$	$.213 \times 10^{-4}$	$.196 \times 10^{-4}$
.52	.472	.485	---	---	.376	.139	---	---
.75	.658	.635	1.174	$.351 \times 10^{-4}$	.469	.398	.367	.346
.98	1.031	.826	---	---	.610	.521	---	---
1.18	1.220	1.080	1.456	.577	.751	.614	.560	.524
1.38	1.220	1.370	---	---	.892	.731	---	---
1.61	1.686	1.620	1.690	.766	1.033	.850	.760	.673
1.86	---	---	---	---	1.174	.956	---	---
2.06	2.254	2.410	1.925	.991	1.362	1.070	.966	.848
2.51	2.819	2.900	2.023	1.230	1.597	1.328	1.132	.996
2.91	3.474	3.460	2.395	1.418	1.878	1.523	1.322	1.139
3.39	4.414	4.350	2.864	1.933	2.019	1.786	1.575	1.324
3.80	5.448	5.520	3.146	2.008	2.535	2.042	1.811	1.517
4.28	6.761	6.570	3.381	2.344	2.951	2.321	2.021	1.674
4.70	8.071	7.830	3.662	2.598	3.333	2.629	2.231	1.821
5.15	9.204	8.780	3.991	2.836	3.662	2.849	2.359	1.922
5.59			4.273	3.188	4.266	3.340	2.611	2.097
6.05			4.742	3.501			2.823	2.244
6.47			---	---			3.080	2.421
6.96			5.587	4.179			3.354	2.604
7.40			---	---			3.609	2.792
7.90			6.433	4.895			3.855	2.988
8.33			---	---			4.129	3.180
8.82			7.606	5.961			---	---
9.28			---	---			4.532	3.566
9.76			8.405	7.015			---	---
10.20			---	---			5.087	3.957
10.41			9.860	5.961			---	---
10.90			14.649				---	---
11.13			---				6.104	4.411
11.33			15.776				---	---
12.05							7.137	4.668

[1]Gage length taken as entire length of specimen.
[2]Gage length taken in middle of specimen.
[3]Questionable data.

TABLE VI

UNIT-TWIST DATA FOR STIFFENED D-TUBES WITH NACA 0012 SECTION - Continued

Torsional moment (in-lb)	Unit twist (radian/in.) for specimen -							
	25 (1)	25 (2)	28 (1)	28 (2)	31 (1)	31 (2)	37 (1) (3)	37 (2) (3)
0	0	0	0	0	0	0	0	0
.150 × 10^4	.09 × 10^-4	.1363 × 10^-4	----------	----------	----------	----------	.195 × 10^-4	.189 × 10^-4
.310	.28	.251	----------	----------	----------	----------	.307	.459
.480	.47	.375	----------	----------	----------	----------	.439	.473
.670	.564	.464	.563 × 10^-4	.351 × 10^-4	.657 × 10^-4	.707 × 10^-4	.583	.531
.840	.751	.550	.798	.486	----------	----------	.709	.660
1.025	.939	.619	.986	.666	.939	.872	.844	.766
1.210	1.127	.709	1.080	.814	----------	----------	.998	.892
1.380	1.221	.793	1.174	.873	1.268	1.156	1.139	1.018
1.560	1.409	.868	1.361	1.055	----------	----------	1.301	1.142
1.740	1.597	.976	1.503	1.210	1.549	1.468	1.448	1.260
1.930	1.898	1.104	1.690	1.342	----------	----------	1.581	1.373
2.120	2.629	1.861	1.878	1.507	2.019	1.766	1.779	1.491
2.200	3.944		----------	----------	----------	----------	1.992	1.669
2.290	5.071		2.159	1.696	----------	----------	2.293	2.179
2.475	1.269		2.300	1.975	2.253	2.173	2.999	2.568
2.568			----------	----------	----------	----------	3.738	3.403
2.820			2.914	2.701	2.817	2.612	4.772	4.543
3.200			3.991	5.088	3.709	3.306	6.199	5.884
3.570			6.244	4.303	4.226	3.976		
3.780			8.263		----------	----------		
3.920			9.578		5.617	4.623		
4.050			10.987		----------	----------		
4.130					7.418	5.245		
4.510					9.531			
4.700					11.268			
4.850					13.428			
	29 (1)	29 (2)	32 (1)	32 (2)	34 (1) (3)	34 (2) (3)	35 (1)	35 (2)
0	0	0	0	0	0	0	0	0
.30 × 10^4	.186 × 10^-4	.224 × 10^-4	.228 × 10^-4	.225 × 10^-4	.376 × 10^-4	.400 × 10^-4	.239 × 10^-4	.220 × 10^-4
.52	.367	.354	----------	----------	.565	.556	----------	----------
.75	.526	.525	.465	.434	.844	.760	.480	.478
.98	.646	.616	----------	----------	1.034	.947	----------	----------
1.18	.766	.721	.708	.422	1.223	1.140	.713	.674
1.38	.871	.833	----------	----------	1.407	1.374	----------	----------
1.61	1.055	.963	1.077	.905	1.596	1.620	.926	.955
1.86	1.175	1.060	----------	----------	----------	----------	----------	----------
2.06	1.328	1.201	1.237	1.163	2.067	1.857	1.258	1.175
2.26	1.439	1.336	----------	----------	----------	----------	----------	----------
2.51	1.698	1.461	1.603	1.499	2.440	2.403	1.527	1.444
2.74	1.785	1.560	----------	----------	----------	----------	----------	----------
2.91	1.860	1.674	1.655	1.564	2.912	2.750	1.755	1.578
3.15	2.001	1.838	----------	----------	----------	----------	----------	----------
3.39	2.212	1.838	1.945	1.813	3.570	3.428	2.087	1.918
3.62	2.389	2.153	----------	----------	----------	----------	----------	----------
3.80	2.572	2.290	2.268	2.142	5.166	4.277	2.356	2.121
4.03	2.701	2.405	----------	----------	----------	----------	----------	----------
4.28	2.873	2.464	2.553	2.406	5.634	5.143	2.638	2.391
4.50	3.050	2.663	----------	----------	----------	----------	----------	----------
4.70	3.176	2.808	2.789	2.649	6.668	6.042	2.891	2.594
4.90	3.333	2.923	----------	----------	----------	----------	----------	----------
5.15	3.456	3.033	3.027	2.819	7.795		3.131	2.771
5.38	3.594	3.163	----------	----------	----------		----------	----------
5.59	3.768	3.286	3.394	3.264	8.339		3.457	2.740
5.80	3.825	3.411	----------	----------	----------		----------	----------
6.05	4.111	3.573	3.690	3.326			3.795	3.283
6.28	4.258	3.707	----------	----------			----------	----------
6.47	5.361	3.813	4.046	3.585			4.118	3.505
6.96			4.798	3.804			4.445	3.791
7.40			6.064	3.769			4.776	4.008
7.90			6.616	3.994			5.153	4.279
8.33			7.367				5.555	4.630
8.82			8.639				5.921	4.538
9.28			9.297				6.303	4.665
9.48							7.090	
10.00							7.559	
10.41							8.170	
10.90							8.687	
11.33							9.297	
11.84							10.001	
12.27							10.752	

[1]Gage length taken as entire length of specimen.
[2]Gage length taken in middle of specimen.
[3]Questionable data.

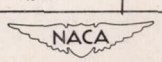

TABLE VI

UNIT-TWIST DATA FOR STIFFENED D-TUBES WITH NACA 0012 SECTION - Continued

Torsional moment (in-lb)	Unit twist (radian/in.) for specimen -							
	38 (1)	38 (2)	39 (1)	39 (2)	41 (1) (3)	41 (2) (3)	43 (1)	43 (2)
0	0	0	0	0	0	0	0	0
$.30 \times 10^4$	$.249 \times 10^{-4}$	$.268 \times 10^{-4}$	$.207 \times 10^{-4}$	$.189 \times 10^{-4}$	$.338 \times 10^{-4}$	$.475 \times 10^{-4}$	$.415 \times 10^{-4}$	$.480 \times 10^{-4}$
.52	.346	.361	---	---	---	---	.557	.586
.75	.436	.446	.334	.293	.441	.505	.688	.723
.98	.562	.564	---	---	---	---	.908	.916
1.18	.694	.681	.505	.469	.649	.757	1.091	1.124
1.38	.817	.786	---	---	---	---	1.259	1.278
1.61	1.025	.925	.745	.655	.954	1.012	1.503	1.522
1.86	1.109	1.040	---	---	---	---	1.691	1.716
2.06	1.250	1.155	.953	.778	1.236	1.356	1.908	1.924
2.51	1.533	1.403	1.181	.978	1.473	1.547	2.421	2.300
2.91	1.755	1.597	1.385	1.073	1.695	1.755	2.840	2.753
3.39	2.079	1.866	1.659	1.274	1.996	2.038	3.163	3.479
3.80	2.422	2.139	1.917	1.436	2.268	2.272	4.375	4.517
4.28	2.744	2.423	2.173	1.591	2.630	2.736	5.154	5.383
4.70	3.116	2.687	2.404	1.734	2.900	2.793	6.190	6.271
5.15	3.495	2.953	2.620	1.849	3.132	3.229	7.231	7.304
5.59	4.186	3.508	2.873	2.021	3.474	3.286	8.545	9.569
5.80	9.649	5.546	---	---	---	---	---	
6.05			3.143	2.167	3.770	3.541	13.616	
6.47			3.411	2.326	4.173	3.840		
6.96			3.651	2.495	4.489	4.344		
7.40			3.924	2.660	4.931	4.366		
7.90			---	---	5.359	4.770		
8.33			4.523	3.039	6.104	5.524		
8.82			---	---	6.902	6.100		
9.28			5.090	3.354	7.466	6.595		
9.76			---	---	8.170	7.066		
10.20			5.716	3.783	9.015	7.788		
10.67			---	---	10.001	9.661		
11.13			6.668	4.210	11.269	10.503		
12.05			7.513	4.660				

	44 (1)	44 (2)	46 (1)	46 (2)	47 (1)	47 (2)	50 (1) (3)	50 (2) (3)
0	0	0	0	0	0	0	0	0
$.3 \times 10^4$	$.276 \times 10^{-4}$	$.246 \times 10^{-4}$	$.432 \times 10^{-4}$	$.458 \times 10^{-4}$	$.237 \times 10^{-4}$	$.333 \times 10^{-4}$	$.227 \times 10^{-4}$	$.270 \times 10^{-4}$
.75	---	---	.682	.671	.415	.848	.452	.454
1.18	.748	.701	1.109	1.225	.664	.703	.729	.719
1.61	---	---	1.530	1.576	.914	.905	.961	.947
2.06	1.256	1.167	1.938	2.011	1.178	1.221	1.263	1.184
2.51	---	---	2.392	2.378	1.391	1.458	1.505	1.418
2.91	1.746	1.686	2.828	2.873	1.584	1.623	1.706	1.594
3.39	---	---	3.104	3.263	1.902	1.921	2.050	1.851
3.80	2.389	2.221	4.057	3.856	2.221	2.244	2.421	2.125
4.28	---	---	4.886	4.745	2.482	2.511	2.737	2.376
4.70	2.996	2.711	5.944	5.409	2.930	2.740	3.113	2.586
5.15	---	---	6.707	6.111	3.492	2.950	3.315	2.849
5.59	3.609	3.247	7.888	7.096	3.663	3.505	3.699	3.201
6.05	---	---	8.925	8.279	4.039	3.499	4.129	3.466
6.47	4.312	3.697	11.176	9.455	4.366	3.035	4.456	3.729
6.96	---	---	12.209	11.065	4.694	3.575	4.733	4.364
7.40	5.015	4.279	15.121		5.072	3.986	5.869	4.504
7.90	---	---			5.400	4.281	6.432	4.868
8.33	6.119	5.006			5.776	4.573	---	---
8.40	---	---			---	---	7.935	6.329
8.82	---	---			6.151	4.861	---	---
9.05	---	---			---	---	12.067	6.699
9.10	---	---			---	---	12.865	7.390
9.28	7.044	5.694			6.527	5.129		
9.76	---	---			6.999	5.475		
10.20	8.264	6.775			7.513	5.759		
11.13	9.673	7.887			8.405	6.625		
12.05	11.551	9.389			9.533	7.109		
12.98					10.989	8.411		
13.88					12.585			
14.84					14.649			
15.78					18.595			
16.25					22.162			

[1]Gage length taken as entire length of specimen.
[2]Gage length taken in middle of specimen.
[3]Questionable data.

TABLE VI

UNIT-TWIST DATA FOR STIFFENED D-TUBES WITH NACA 0012 SECTION - Continued

Torsional moment (in-lb)	Unit twist (radian/in.) for specimen -							
	52 (1)	52 (2)	53 (1) (3)	53 (2) (3)	55 (1) (3)	55 (2) (3)		
0	0	0	0	0	0	0		
$.30 \times 10^4$	$.399 \times 10^{-4}$	$.421 \times 10^{-4}$	$.286 \times 10^{-4}$	$.330 \times 10^{-4}$	$.418 \times 10^{-4}$	$.005 \times 10^{-4}$		
.50	.534	.535	.343	.373	.567	.827		
.73	.699	.668	.473	.476	.737	1.053		
.97	.955	.920	.577	.571	.924	1.575		
1.19	1.155	1.049	.751	.604	1.141	1.583		
1.40	1.354	1.226	.881	.764	1.351	1.823		
1.62	1.610	1.471	1.024	.886	1.601	2.140		
1.86	1.840	1.655	1.168	.982	1.823	2.431		
2.06	2.123	1.934	1.311	1.088	2.052	2.711		
2.26	2.353	2.152	---	---	2.255	2.891		
2.50	2.635	2.418	1.580	1.309	2.485	3.083		
2.92	3.373	3.016	1.897	1.555	2.945	3.499		
3.37	4.184	3.242	2.261	1.891	3.650	4.100		
3.81	5.144	4.504	2.565	2.085	4.720	5.148		
4.26	6.316	5.420	2.886	3.269	5.810	6.250		
4.50	8.308	7.759	---	---	---	---		
4.70	8.842	8.302	3.199	2.471	6.710	7.563		
5.15			3.550	2.676	8.135	8.425		
5.59			3.997	2.935	11.380	10.150		
6.05			---	---	13.230	10.975		
6.50			4.740	3.410				
6.95			---	---				
7.42			5.495	3.910				
7.89			---	---				
8.35			6.380	4.439				
	36 (1)	36 (2)	45 (1) (3)	45 (2) (3)	54 (1) (3)	54 (2) (3)	57 (1) (3)	57 (2) (3)
0	0	0	0	0	0	0	0	0
$.098 \times 10^4$	$.1713 \times 10^{-4}$	$.05 \times 10^{-4}$	$.502 \times 10^{-4}$	$.475 \times 10^{-4}$	$.208 \times 10^{-4}$	$.168 \times 10^{-4}$	$.123 \times 10^{-4}$	$.100 \times 10^{-4}$
1.50	.6725	.413	1.079	.941	.516	.680	.614	.520
3.60	1.1992	.938	1.520	1.357	1.033	.864	1.145	.954
5.00	---	---	2.016	1.808	1.576	1.260	1.676	1.424
6.05	2.1785	1.75	2.656	2.368	1.775	1.713	2.223	1.881
7.20	---	---	3.173	2.807	3.073	2.185	2.815	2.323
8.40	3.4570	2.725	3.810	3.324	4.023	2.716	3.631	2.888
9.50	4.0549	3.225	4.360	3.781	4.661	3.171	4.284	3.358
11.10	4.8617	3.725	5.066	4.331	5.755	3.676	4.999	3.866
12.10	5.6069	4.375	6.010	4.808	6.693	4.251	5.731	4.368
13.25	6.6241	4.725	6.806	5.348	7.478	4.689	6.340	4.773
14.80	---	---	7.561	5.829	8.238	5.248	6.966	5.258
15.90	8.1219	5.625	8.077	6.233	9.089	5.608	7.642	5.758
17.20	---	---	8.826	6.693	10.104	6.088	---	---
18.25	9.2037	6.487	9.766	7.364	10.716	6.424	9.424	6.548
19.60	---	---	10.707	8.114	11.871	7.201	---	---
20.80	10.7542	7.80	---	---	12.821	7.759	11.088	7.683
22.05	11.6436	8.188	13.147	9.845	---	---	---	---
23.20	---	8.913			15.260	8.871	12.932	8.934
24.30	13.7560	9.4			16.684	9.935	---	---
25.80	14.5923	10.26			18.585	12.516	17.629	11.304
27.00	17.7043							

[1]Gage length taken as entire length of specimen.
[2]Gage length taken in middle of specimen.
[3]Questionable data.

TABLE VI

UNIT-TWIST DATA FOR STIFFENED D-TUBES WITH NACA 0012 SECTION - Concluded

Torsional moment (in-lb)	Unit twist (radian/in.) for specimen -			
	40 (1) (3)	40 (2) (3)	49 (1) (3)	49 (2) (3)
0	0	0	0	0
$.310 \times 10^4$	$.338 \times 10^{-4}$	$.380 \times 10^{-4}$	$.295 \times 10^{-4}$	$.325 \times 10^{-4}$
.670	.601	.719	.545	.600
.850	---	---	.689	.719
1.020	.847	1.000	.828	.856
1.210	---	---	.983	1.012
1.380	1.126	1.309	1.160	1.172
1.560	---	---	1.352	1.268
1.740	1.435	1.640	1.529	1.400
1.930	---	---	1.730	1.549
2.110	1.785	1.959	1.918	1.661
2.300	---	---	2.118	1.767
2.480	2.153	2.919	2.310	1.870
2.660	---	---	2.539	2.035
2.850	2.501	2.570	2.835	2.148
3.030	2.765	2.911	3.040	2.273
3.220	3.004	3.242	3.263	2.485
3.390	3.302	3.438	3.750	3.200
3.580	3.640	3.801	4.085	3.520
3.680	3.900	4.123	4.440	3.772
3.960	4.270	4.418	4.440	4.150
4.150	5.124		7.680	4.470
4.350	5.608		7.680	4.510
4.400	6.250			4.870
4.500	---			5.400
4.700	7.014			6.280
4.880	7.907			
5.070	9.438			
5.220	10.236			
	55 (1) (3)	55 (2) (3)	56 (1)	56 (2)
0	0	0	0	0
$.30 \times 10^4$	$.418 \times 10^{-4}$	$.605 \times 10^{-4}$	$.265 \times 10^{-4}$	$.219 \times 10^{-4}$
.52	.567	.827	---	---
.75	.737	1.053	.489	.490
.98	.924	1.575	---	---
1.18	1.141	1.583	.786	.741
1.38	1.351	1.823	---	---
1.61	1.601	2.140	1.111	1.088
1.86	1.823	2.431	---	---
2.06	2.052	2.711	1.452	1.230
2.26	2.255	2.891	---	---
2.51	2.485	3.083	1.758	1.450
2.91	2.945	3.499	2.042	1.664
3.39	3.650	4.100	2.506	2.013
3.80	4.720	5.148	2.949	2.286
4.28	5.810	6.250	3.390	2.540
4.70	6.710	7.563	3.803	2.830
5.15	8.135	8.425	4.196	3.040
5.59	11.380	10.150	4.672	3.330
6.05	13.230	10.975	5.170	3.630
6.47			5.717	3.890
6.96			6.122	4.160
7.40			6.628	4.480
8.33			7.367	5.120
9.28			8.669	5.700
10.20			10.868	8.490
11.13			12.310	9.730
12.05			14.127	11.230
12.98			21.903	

[1]Gage length taken as entire length of specimen.

[2]Gage length taken in middle of specimen.

[3]Questionable data.

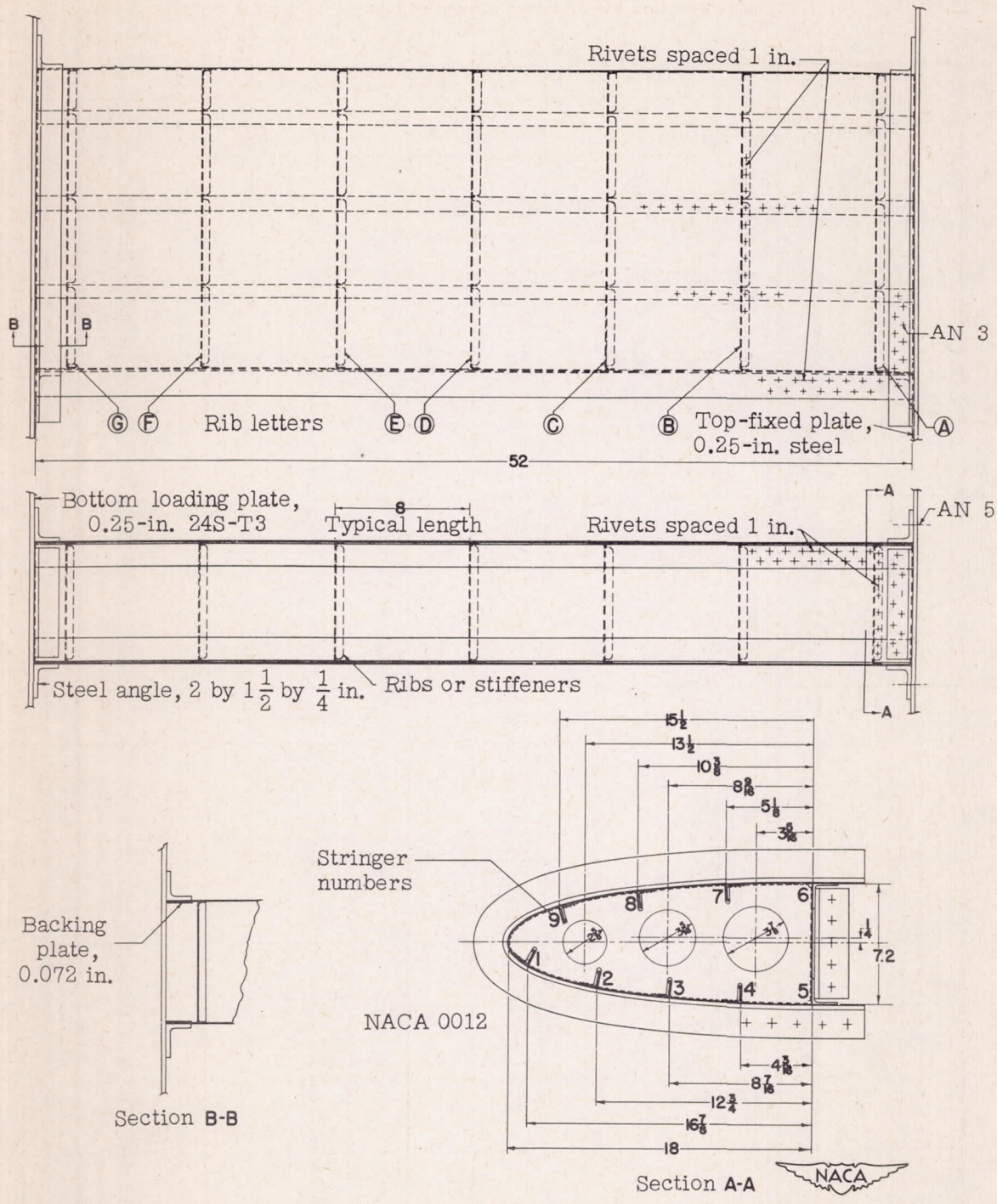

Figure 1.- Details of specimen 48; dimensions given in inches. Other specimens similar except for number of ribs and stringers. Dimensions vary with specimen; see table I.

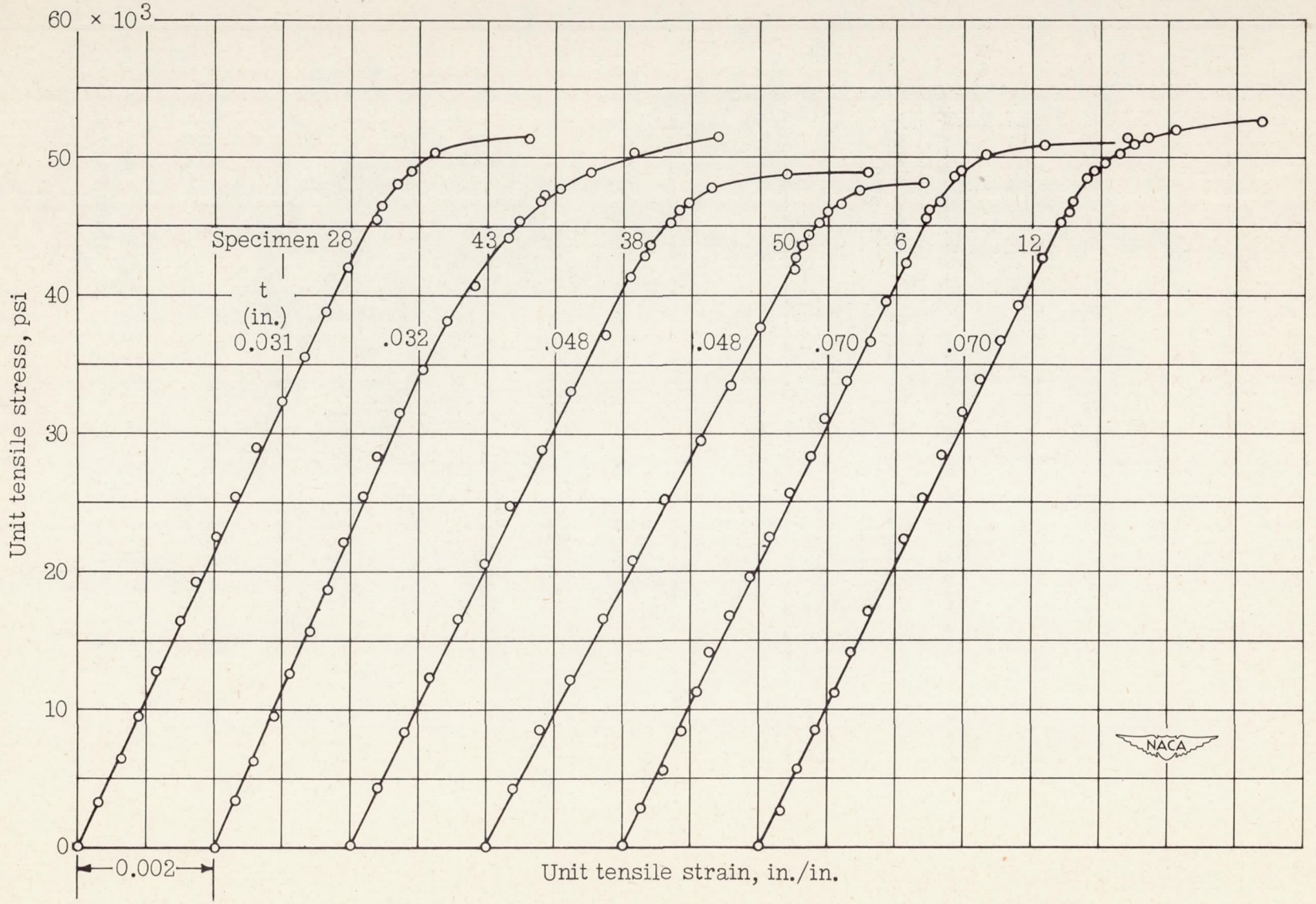

Figure 2.- Typical stress-strain curves for alclad 24S-T3 aluminum-alloy skin material.

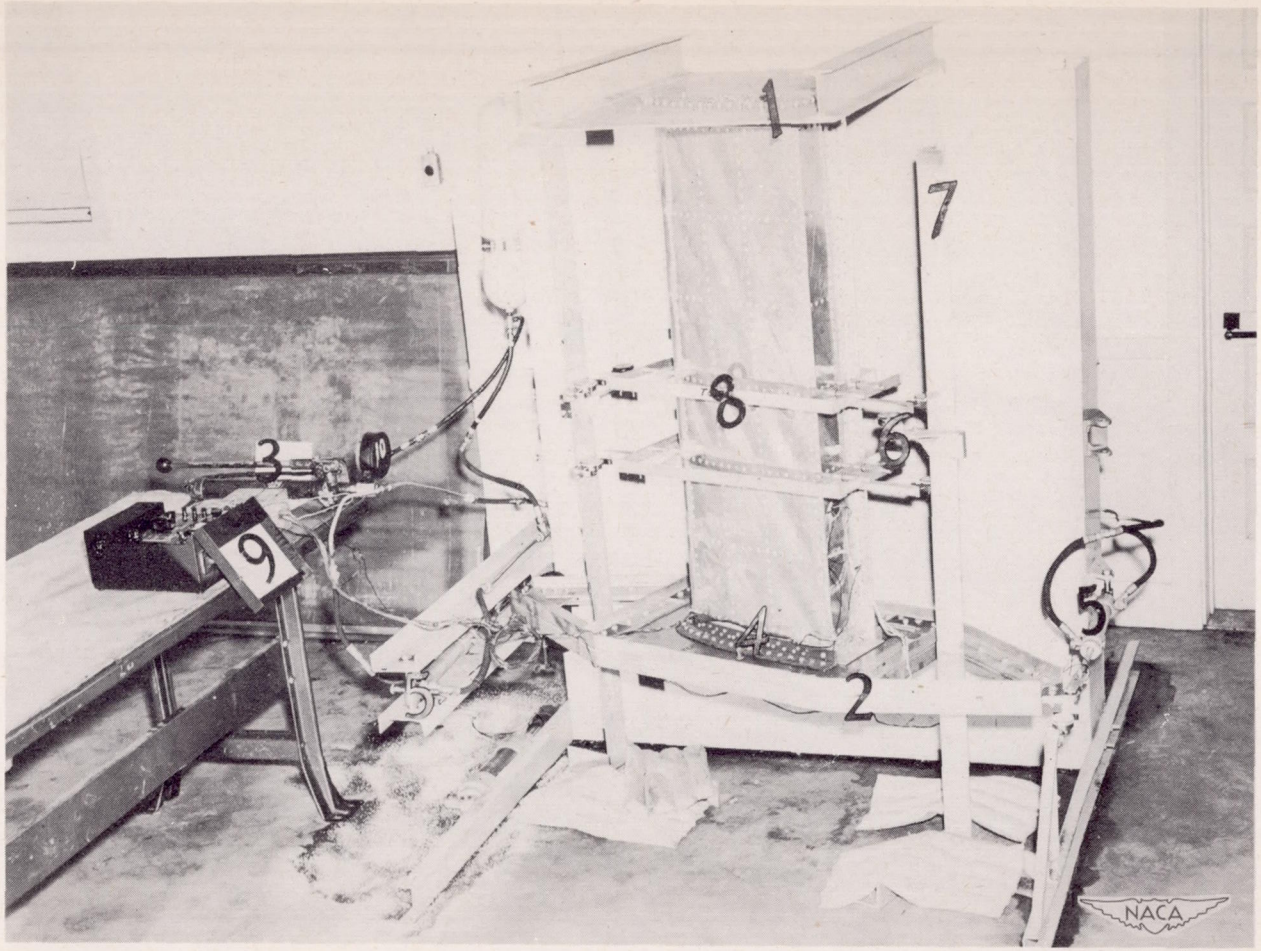

Figure 3.- Specimen in place in apparatus used to load specimen in torsion. 1, top loading plate; 2, bottom loading plate; 3, hand pump for operating pistons; 4, steel angles to which specimen was bolted; 5, hydraulic pistons by which load was applied; 6, dial gages; 7, vertical columns; 8, rectangular frames used with 6 and 7 to obtain twist data; 9, strain boxes, type K.

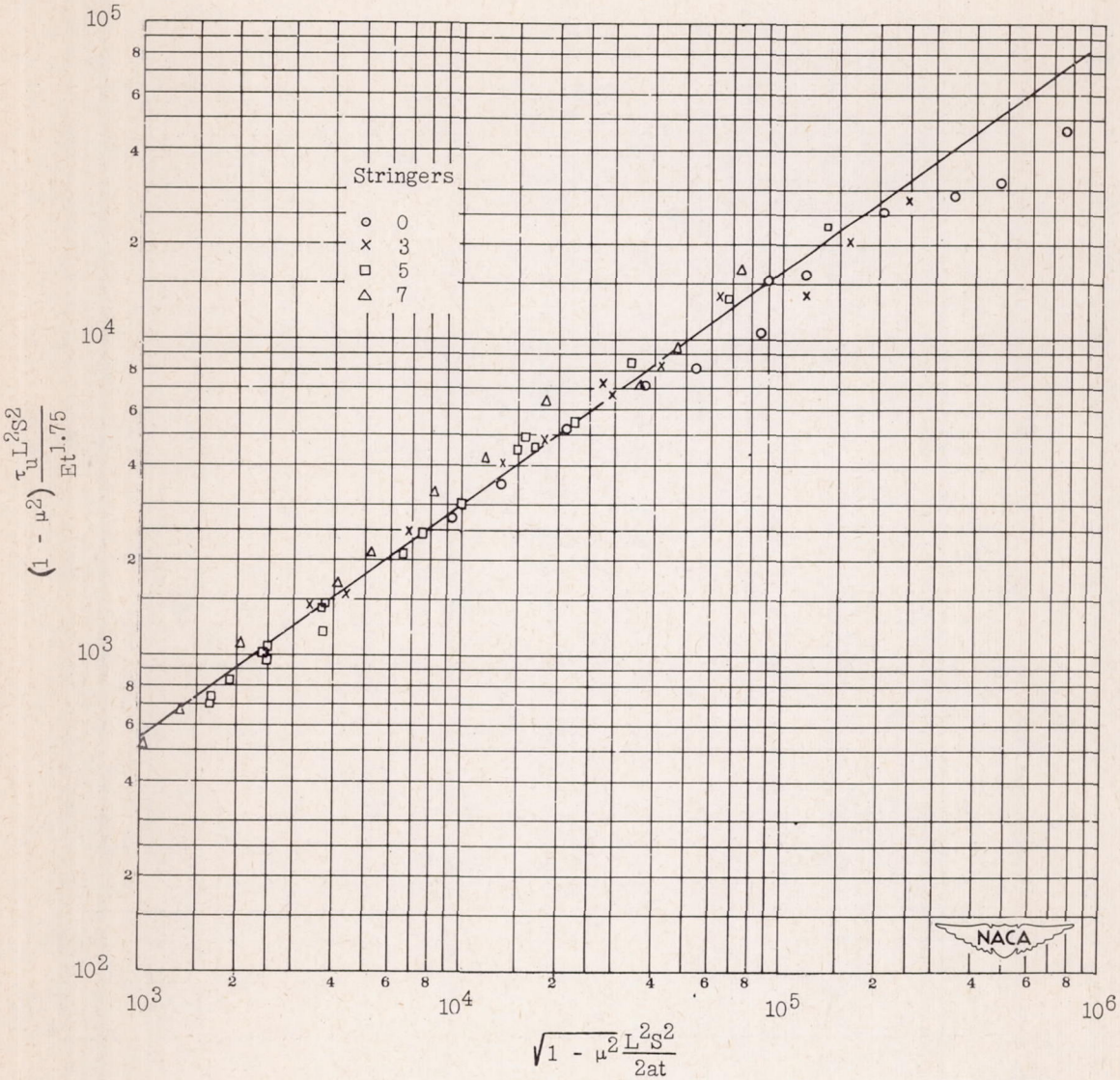

Figure 4.- Curve of average ultimate torsional strength of D-tubes with NACA 0012 section and closing web at 30-percent station plotted from equation (1). Specimens made of alclad 24S-T3 aluminum alloy; $E = 10.2 \times 10^6$ psi, $\mu = 0.33$.

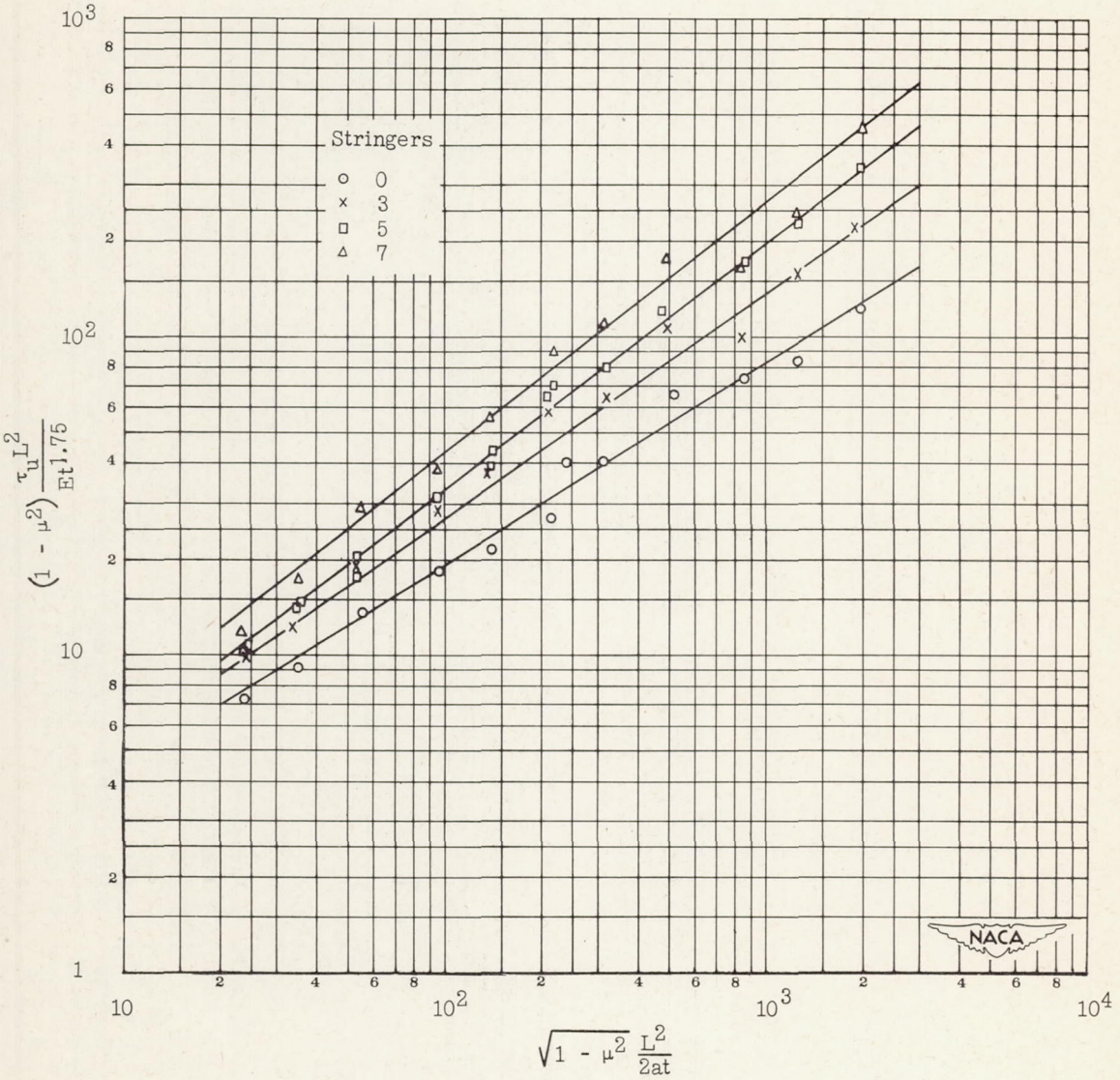

Figure 5.- Ultimate torsional strength of stiffened D-tubes with NACA 0012 section and closing web at 30-percent station. Specimens made of alclad 24S-T3 aluminum alloy; E = 10.2 × 10^6 psi, μ = 0.33.

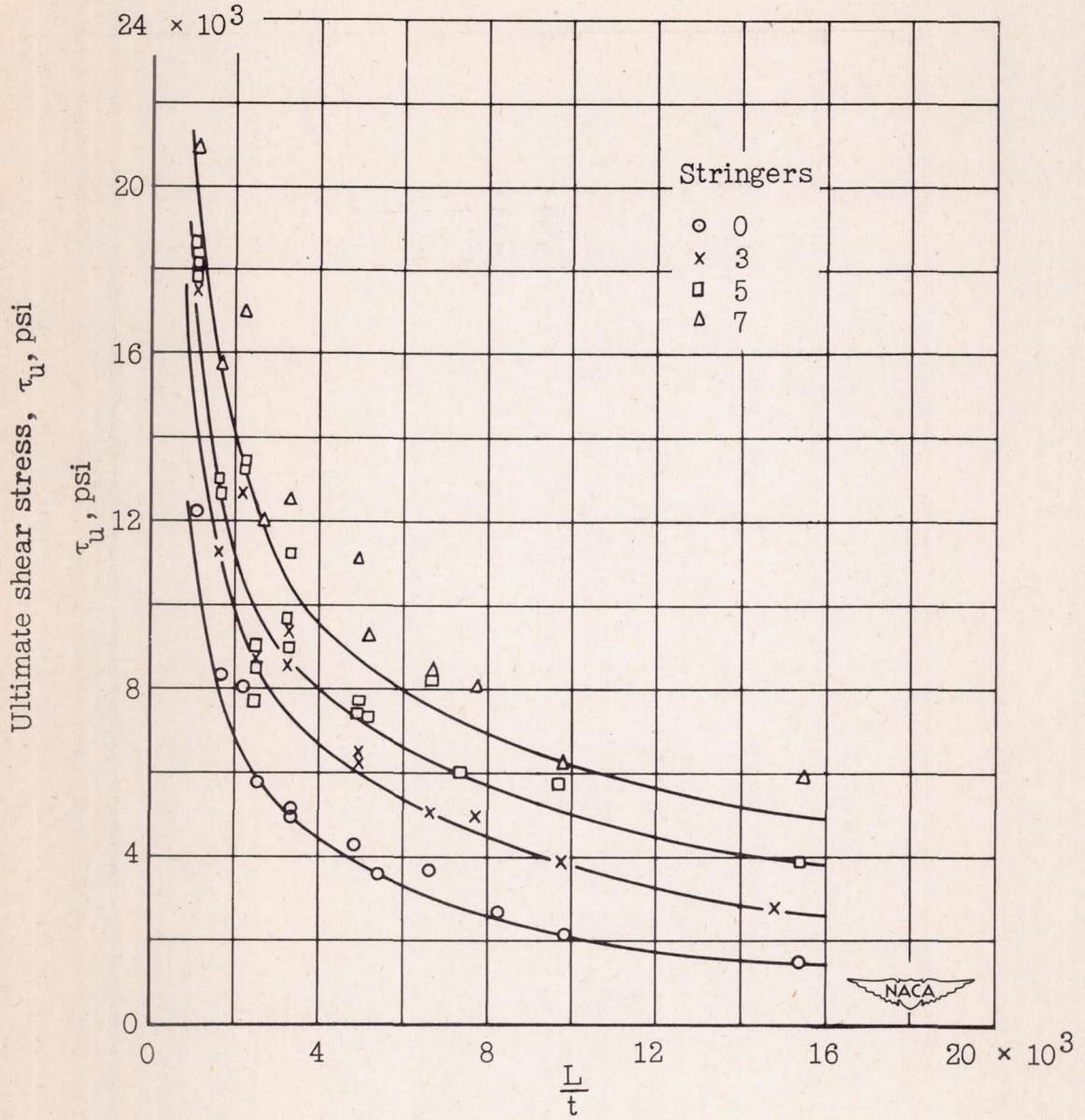

Figure 6.- Average ultimate torsional strength of stiffened D-tubes with NACA 0012 section and closing web at 30-percent station plotted from simplified form of equation (1). Specimens made of alclad 24S-T3 aluminum alloy; E = 10.2 × 10^6 psi, μ = 0.33.

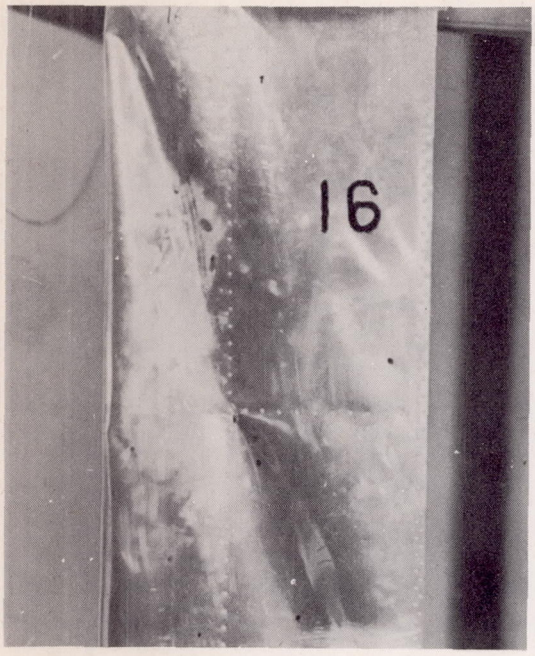

(a) Failure at intersection of rib and stringer.

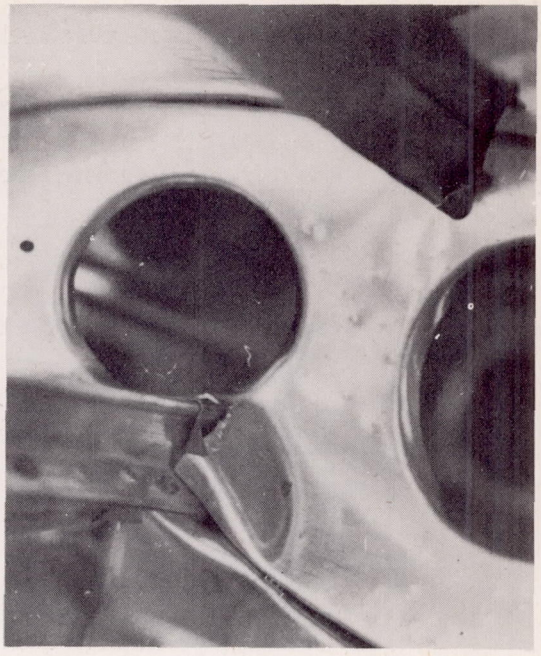

(b) Close-up view of failure at intersection of rib and stringer.

(c) Failure produced by collapse of nose section.

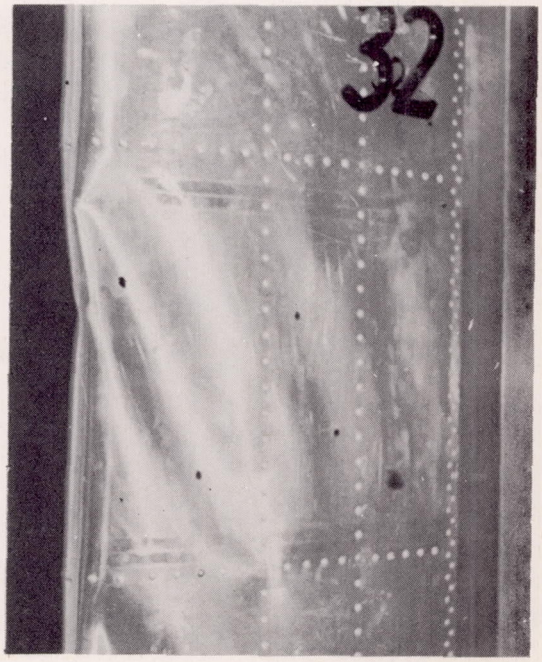

(d) Close-up view of failure produced by collapse of nose section.

NACA

Figure 7.- Some typical failures encountered in tests of stiffened D-tubes.

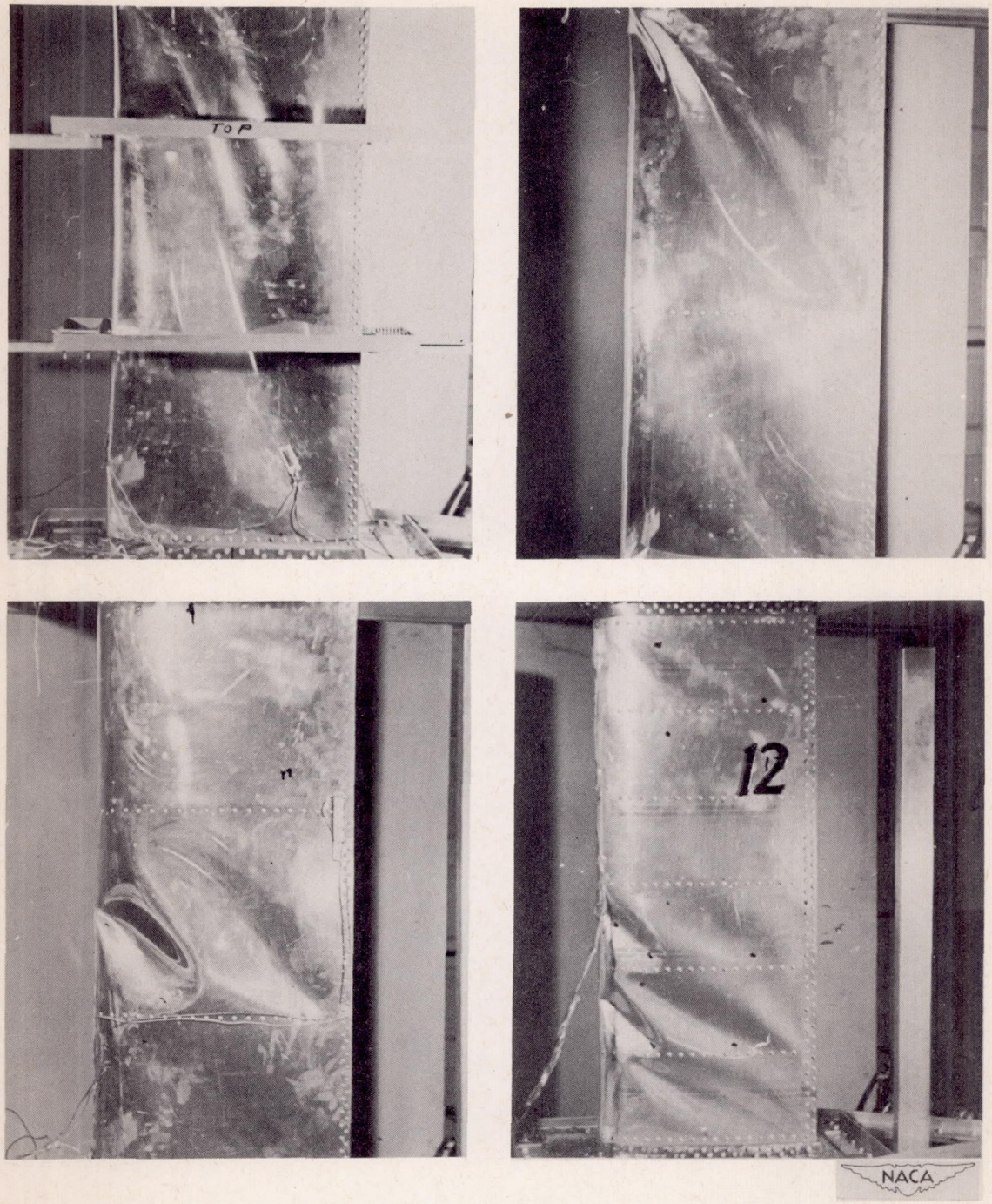

Figure 8.- Patterns of wrinkles at failure for specimens without stringers.

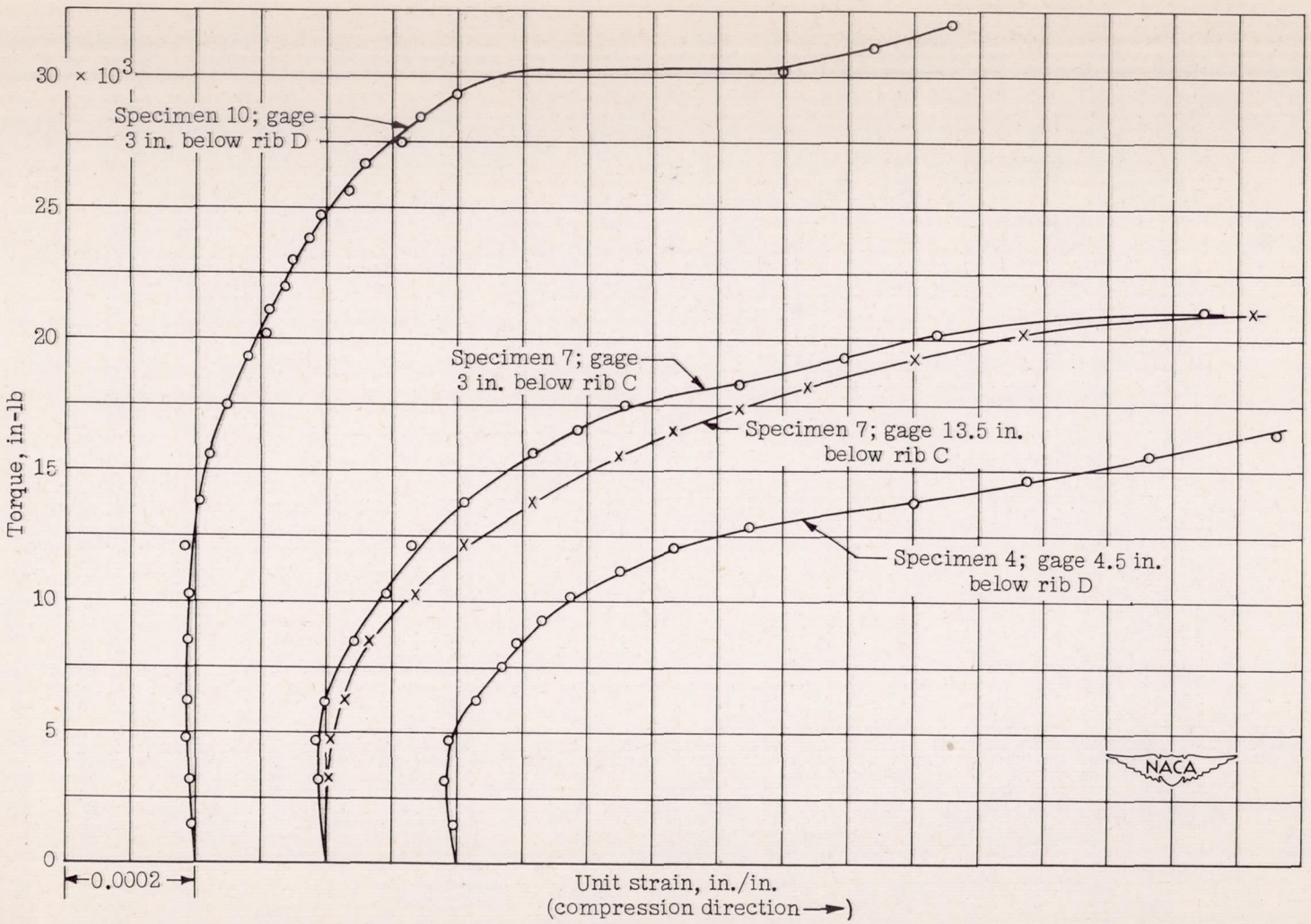

Figure 9.- Development of longitudinal unit strain in nose of stiffened D-tubes with NACA 0012 section and closing web at 30-percent station. Specimens made of alclad 24S-T3 aluminum alloy; $E = 10.2 \times 10^6$ psi, $\mu = 0.33$, $t = 0.031$ inch. See figure 1 for rib positions.

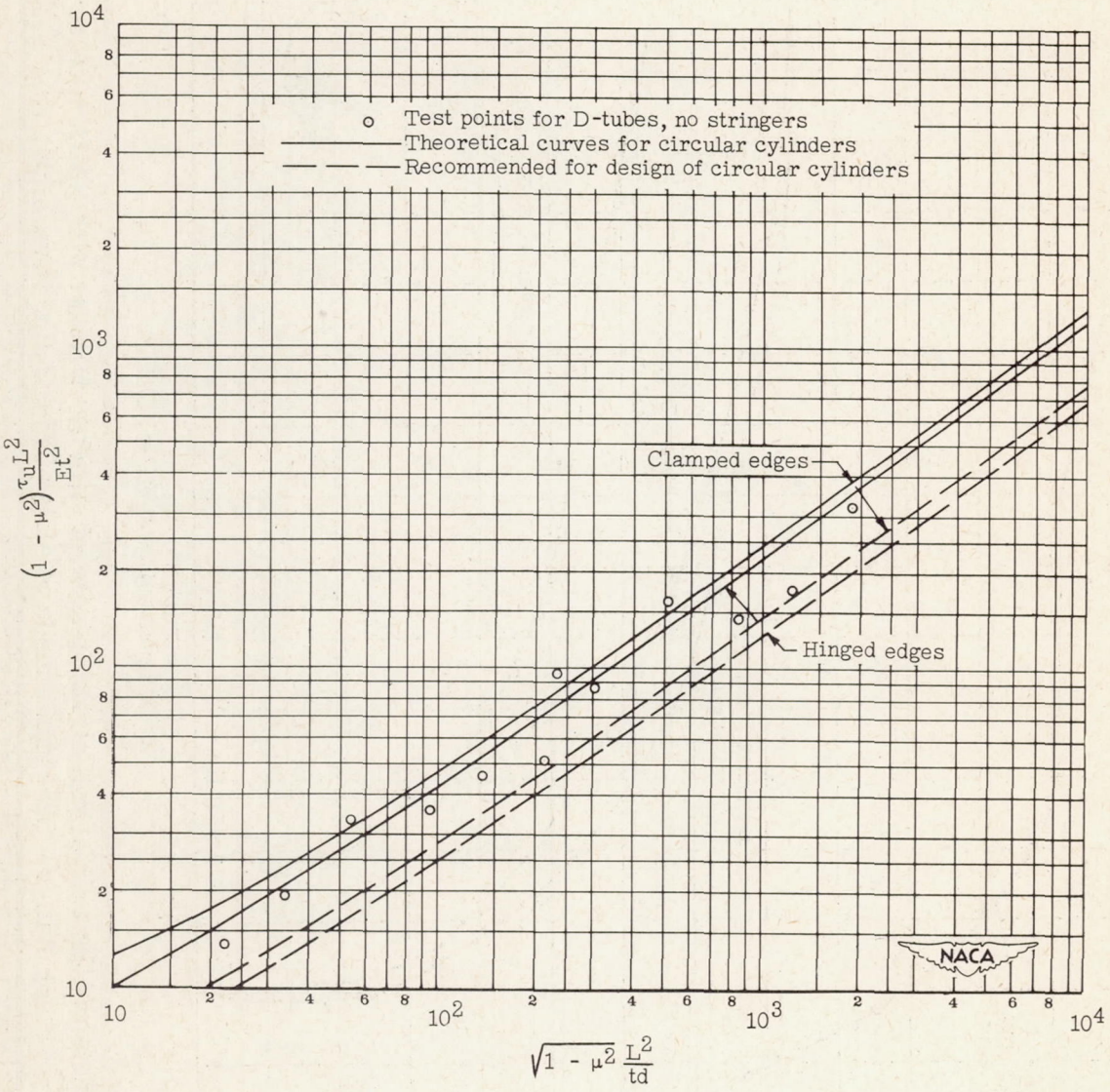

Figure 10.- Comparison of critical torsional stress for circular cylinders and D-tubes. Short and medium-length tubes tested; diameter d of circular cylinders taken as 2a for D-tubes.

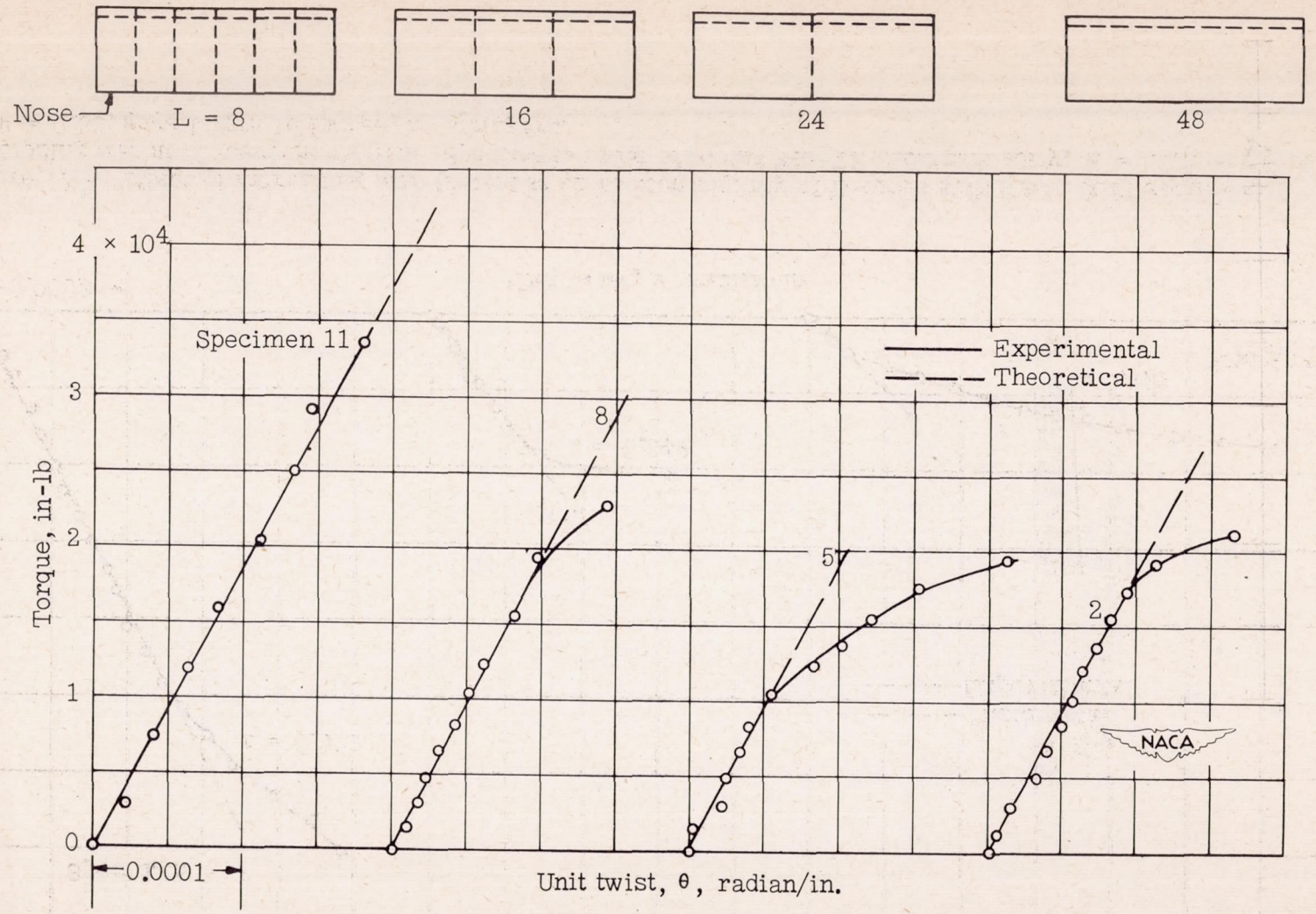

Figure 11.- Experimental and theoretical values of torsional stiffness of D-tubes having no stringers with NACA 0012 section and closing web at 30-percent station. Specimens made of alclad 24S-T3 aluminum alloy; E = 10.2 × 10^6 psi, μ = 0.33, t = 0.049 inch, a = 18 inches.

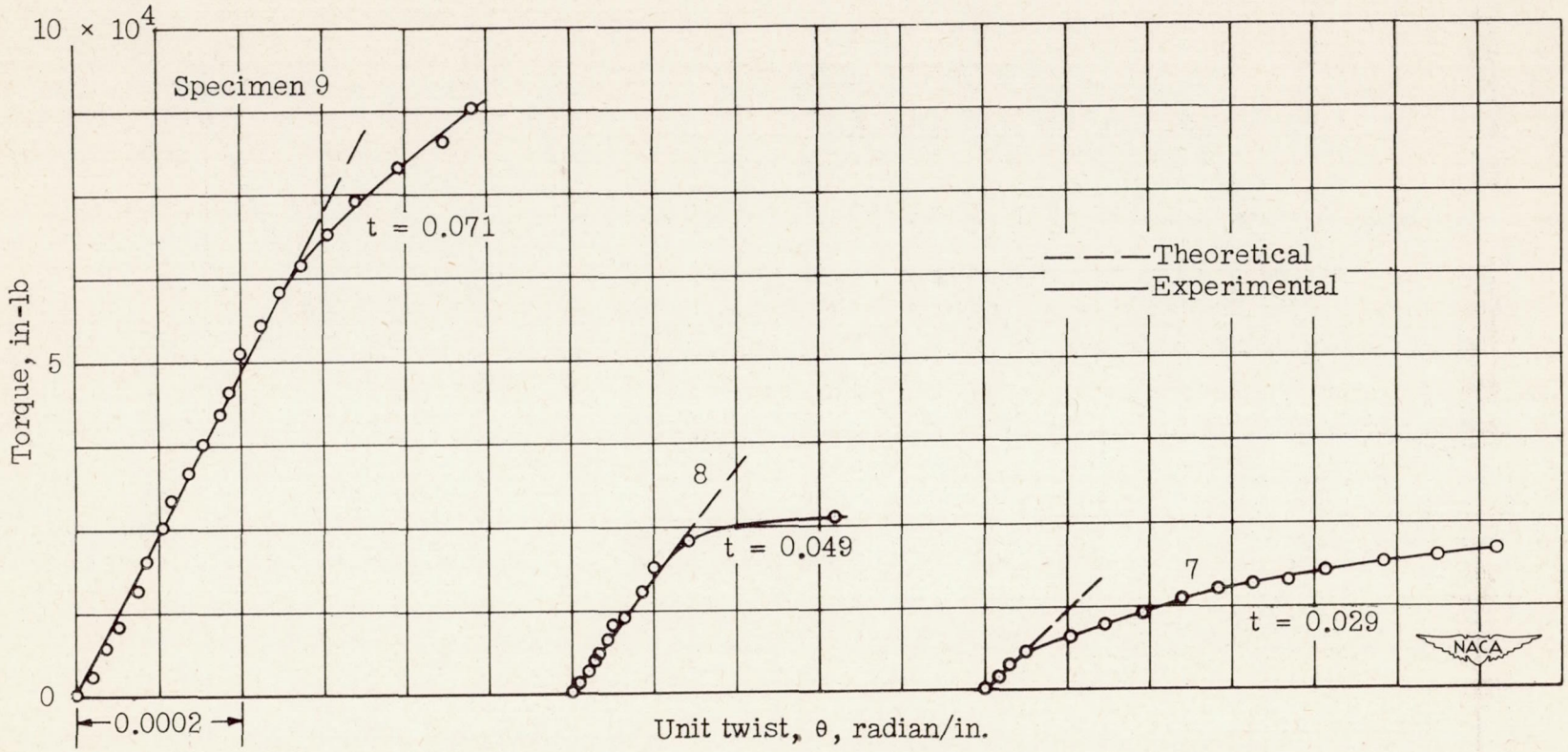

Figure 12.- Effect of increasing skin thickness on section rigidity of D-tubes with NACA 0012 section and closing web at 30-percent station. Specimens made of alclad 24S-T3 aluminum alloy; $E = 10.2 \times 10^6$ psi, $\mu = 0.33$, gage length 16 inches, no stringers.

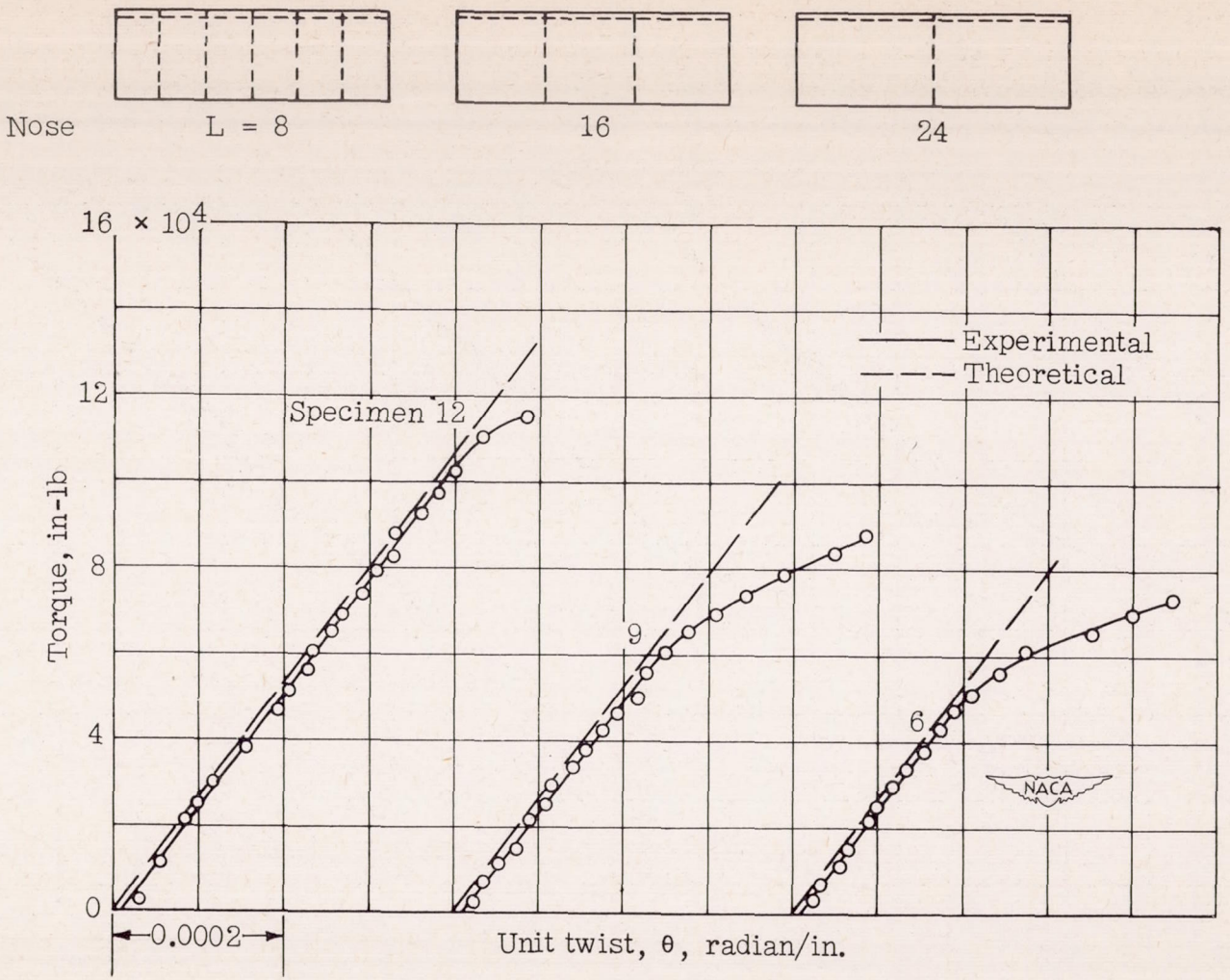

Figure 13.- Experimental and theoretical values of torsional stiffness of D-tubes revealing experimental error encountered during testing. Specimens made of alclad 24S-T3 aluminum alloy with NACA 0012 airfoil section and closing web at 30-percent station; $E = 10.2 \times 10^6$ psi, $\mu = 0.33$, $t = 0.071$ inch, $a = 18$ inches, no stringers.

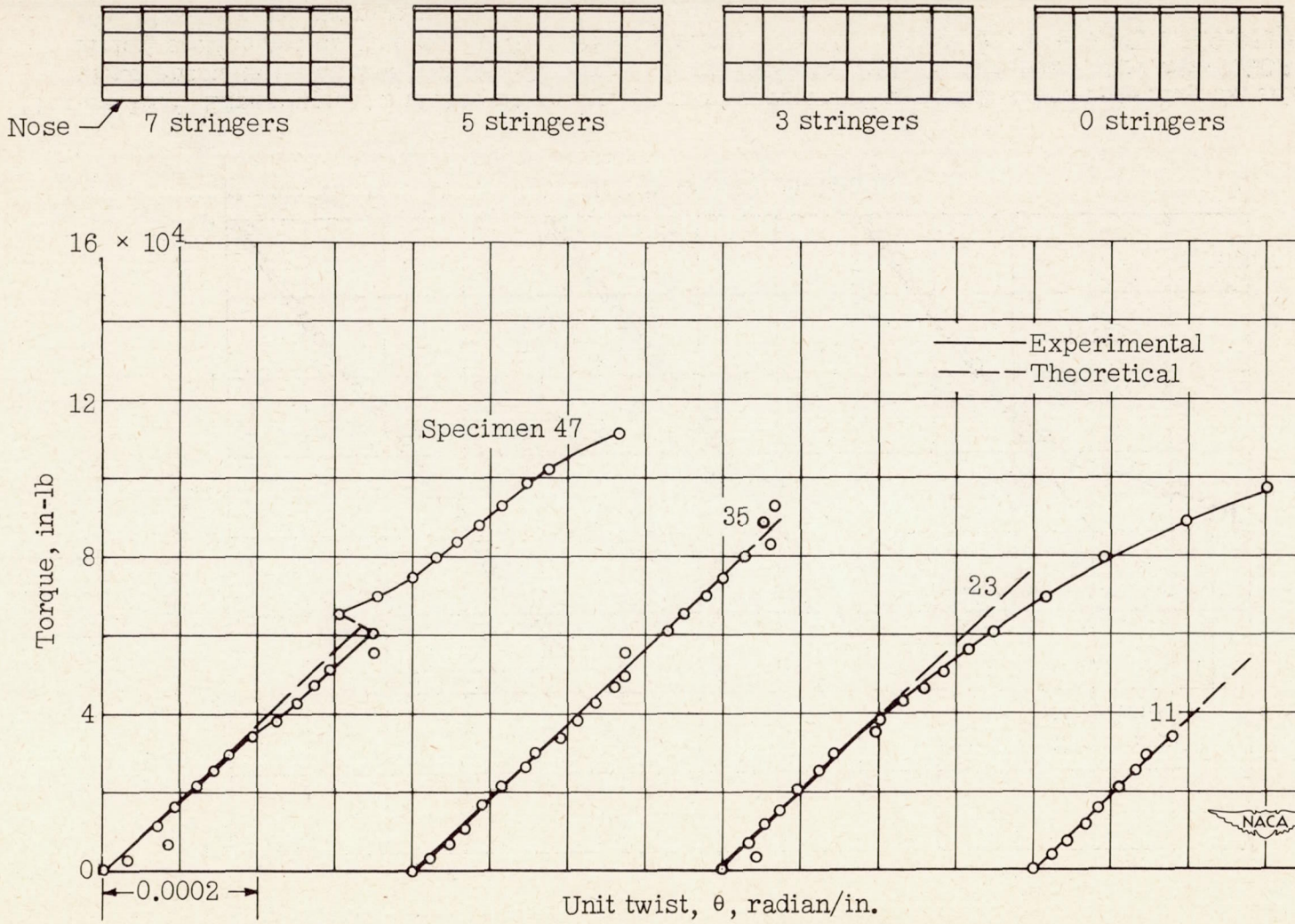

Figure 14.- Effect of addition of stringers on torsional stiffness of D-tubes with NACA 0012 section and closing web at 30-percent station. Specimens made of alclad 24S-T3 aluminum alloy; $E = 10.2 \times 10^6$ psi, $\mu = 0.33$, $t = 0.049$ inch, $a = 18$ inches, $L = 8$ inches.

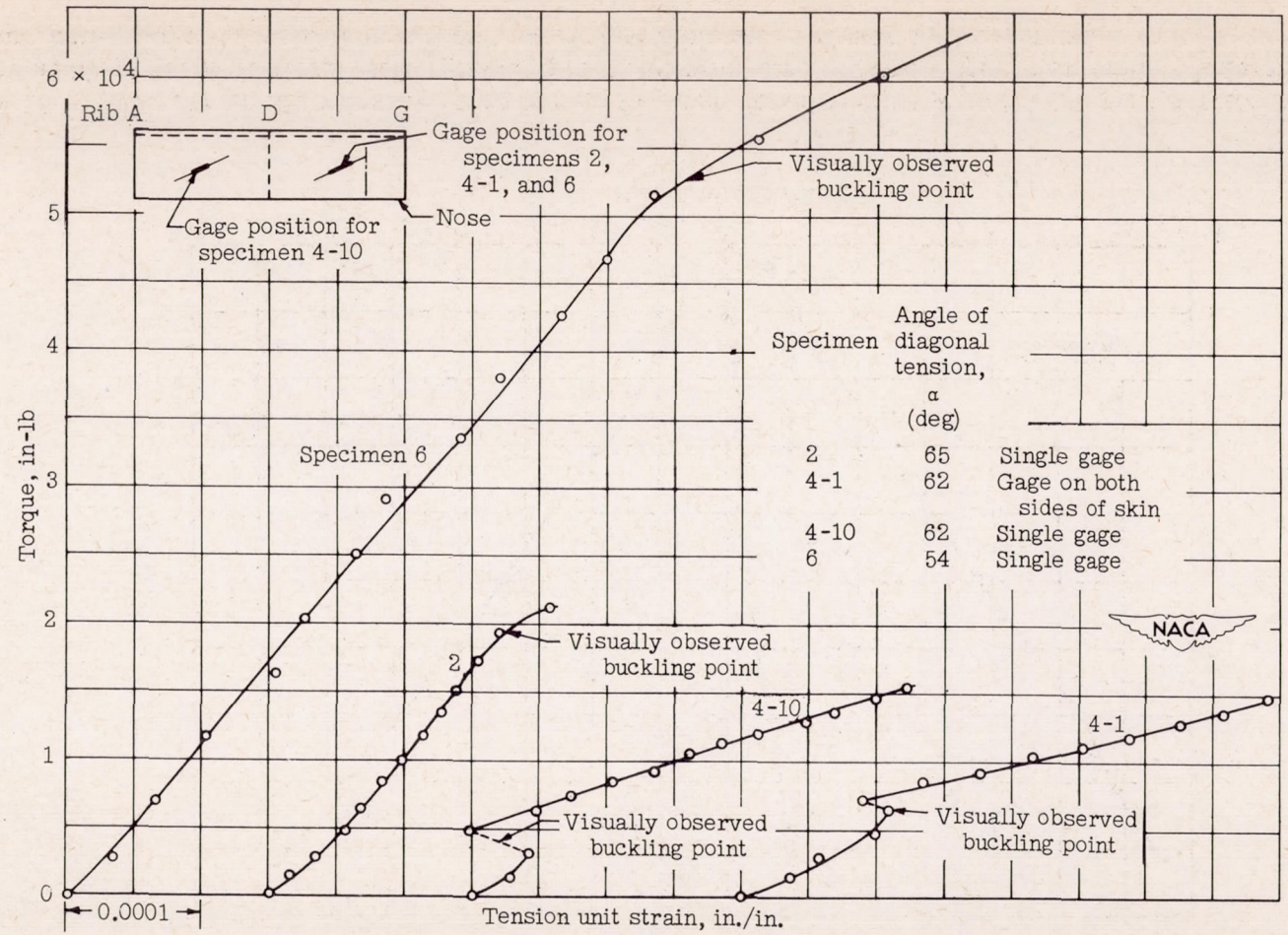

Figure 15.- Skin unit strain in direction of wrinkle of D-tubes with NACA 0012 section and closing web at 30-percent station. Specimens made of alclad 24S-T3 aluminum alloy; $E = 10.2 \times 10^6$ psi, $\mu = 0.33$, $a = 18$ inches, no stringers. Specimen 4-1 denotes specimen 4 with skin panel on which gage 1 was located buckling first; specimen 4-10 denotes specimen 4 with skin panel on which gage 10 was located buckling first.

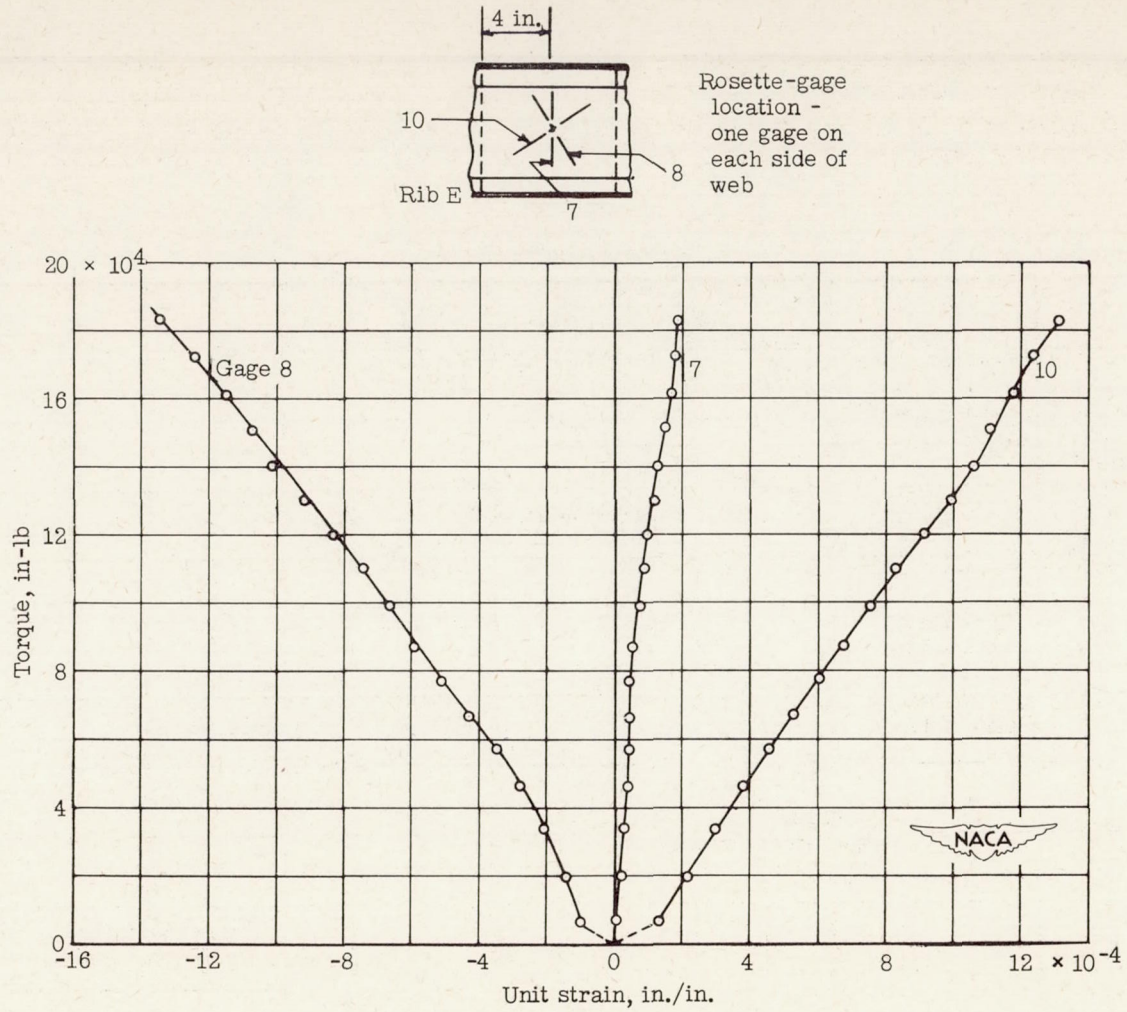

Figure 16.- Web strain distribution of specimen 21, a stiffened D-tube with NACA 0012 section and closing web at 30-percent station. Strain measured on rosette strain gages; specimen made of alclad 24S-T3 aluminum alloy; $E = 10.2 \times 10^6$ psi, $\mu = 0.33$, thickness of web is 0.081 inch.

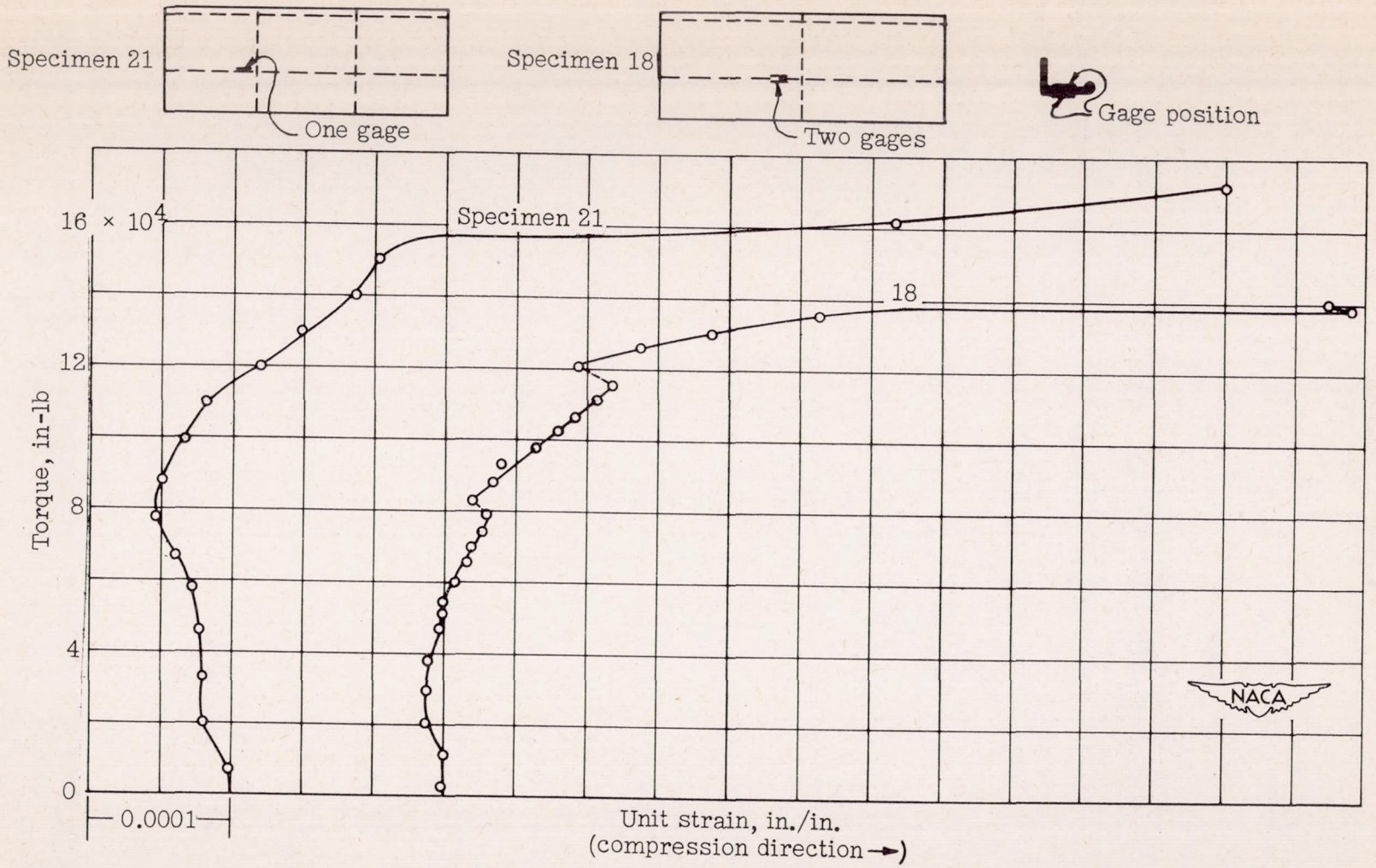

Figure 17.- Stringer unit strain of stiffened D-tubes with NACA 0012 section and closing web at 30-percent station. Skin made of alclad 24S-T3 aluminum alloy; 1- by 7/8- by 0.078-inch bulb-angle stringers made of 24S-T4 aluminum alloy; stringers continuous through ribs; $E = 10.2 \times 10^6$ psi, $\mu = 0.33$, $t = 0.071$ inch.